MicrosporidiaDB: functional genomic resources for Amoebozoa and Microsporidia species. *Nucleic Acids Res* 2011, 39:D612-D619.
42. Chen YH, Su LH, Huang YC, Wang YT, Kao YY, Sun CH: **UPF1, a conserved nonsense-mediated mRNA decay factor, regulates cyst wall protein transcripts in *Giardia lamblia*.** *PLoS ONE* 2008, 3:e3609.
43. Bianchi ME, Agresti A: **HMG proteins: dynamic players in gene regulation and differentiation.** *Curr Opin Genet Dev* 2005, 15:496-506.
44. Abhyankar MM, Hochreiter AE, Hershey J, Evans C, Zhang Y, Crasta O, Sobral BW, Mann BJ, Petri WA Jr, Gilchrist CA: **Characterization of an *Entamoeba histolytica* high-mobility-group box protein induced during intestinal infection.** *Eukaryot cell* 2008, 7:1565-1572.
45. Sikalidis AK, Lee JI, Stipanuk MH: **Gene expression and integrated stress response in HepG2/C3A cells cultured in amino acid deficient medium.** *Amino Acids* 2010, 1-13.
46. Shorer H, Amar N, Meerson A, Elazar Z: **Modulation of N-ethylmaleimide-sensitive factor activity upon amino acid deprivation.** *J Biol Chem* 2005, 280:16219-16226.
47. Li D, Roberts R: **WD-repeat proteins: structure characteristics, biological function, and their involvement in human diseases.** *Cell Mol Life Sci* 2001, 58:2085-2097.
48. Bracha R, Nuchamowitz Y, Anbar M, Mirelman D: **Transcriptional silencing of multiple genes in trophozoites of *Entamoeba histolytica*.** *PLoS Pathog* 2006, 2:e48.
49. Bracha R, Nuchamowitz Y, Mirelman D: **Transcriptional silencing of an amoebapore gene in Entamoeba histolytica: molecular analysis and effect on pathogenicity.** *Eukaryot Cell* 2003, 2:295-305.
50. Vander Ploeg JR, Iwanicka-Nowicka R, Bykowsky T, Hryniewicz N, Leisinger T: **The *Escherichia coli ssuEADCB* gene cluster is required for the utilization of sulfur from aliphatic sulfonates and is regulated by the transcriptional activator Cbl.** *J Biol Chem* 1999, 274:29358-29365.
51. Diamond LS, Harlow DR, Cunnick CC: **A new medium for the axenic cultivation of *Entamoeba histolytica* and other *Entamoeba*.** *Trans R Soc Trop Med Hyg* 1978, 72:431-432.
52. Clark CG, Diamond LS: **Methods for cultivation of luminal parasitic protists of clinical importance.** *Clin Microbiol Rev* 2002, 15:329-341.

doi:10.1186/1471-2164-12-275
Cite this article as: Husain *et al.*: Global analysis of gene expression in response to L-Cysteine deprivation in the anaerobic protozoan parasite *Entamoeba histolytica*. *BMC Genomics* 2011 12:275.

Journal of Antimicrobial Chemotherapy Advance Access published June 14, 2011

J Antimicrob Chemother
doi:10.1093/jac/dkr238

Journal of Antimicrobial Chemotherapy

Mechanism of trifluoromethionine resistance in *Entamoeba histolytica*

Gil M. Penuliar[1–3], Atsushi Furukawa[1,2], Dan Sato[4] and Tomoyoshi Nozaki[1,5]*

[1]*Department of Parasitology, National Institute of Infectious Diseases, 1-23-1 Toyama, Shinjuku-ku, Tokyo 162-8640, Japan;* [2]*Department of Parasitology, Gunma University Graduate School of Medicine, 3-39-22 Showa-machi, Maebashi 371-8511, Japan;* [3]*Institute of Biology, College of Science, University of the Philippines, Diliman, Quezon City 1101, Philippines;* [4]*Institute for Advance Biosciences, Keio University, Tsuruoka, Yamagata 997-0052, Japan;* [5]*Graduate School of Life and Environmental Sciences, University of Tsukuba, 1-1-1 Tennodai, Tsukuba, Ibaraki 305-8572, Japan*

*Corresponding author. Tel: +81-3-52851111, ext. 2600; Fax: +81-3-52851219; E-mail: nozaki@nih.go.jp

Received 16 February 2011; returned 29 March 2011; revised 26 April 2011; accepted 16 May 2011

Objectives: To determine the mechanism of trifluoromethionine resistance in *Entamoeba histolytica* and evaluate the impact of acquired drug resistance on virulence.

Methods: Trifluoromethionine-resistant amoebae were selected *in vitro* and examined for cross-resistance to antiamoebic drugs, stability of resistance, methionine γ-lyase (MGL) activity, cell adhesion and virulence. Targeted gene silencing was performed to confirm the role of *Eh*MGL.

Results: Trophozoites with a resistance index of 154 were obtained. The cells were susceptible to chloroquine, metronidazole, paromomycin and tinidazole, but remained resistant to trifluoromethionine in the absence of drug pressure. A complete lack of *Eh*MGL activity accompanied by increased adhesion and decreased cytolysis were also observed. Silencing of the *Eh*MGL genes resulted in trifluoromethionine resistance.

Conclusions: This study provides the first demonstration of trifluoromethionine resistance in a parasitic protozoon. Repression of gene expression of drug targets represents a novel mechanism of resistance in *E. histolytica*. The information obtained from this work should help further development of trifluoromethionine derivatives that have lower chances of inducing resistance.

Keywords: amoebiasis, drug resistance, methionine γ-lyase

Introduction

Amoebiasis is an intestinal disease affecting 50 million people each year. Responsible for 110 000 deaths annually, it occupies an important place on the list of parasitic causes of mortality worldwide.[1] The aetiological agent is *Entamoeba histolytica*, and is contracted through the ingestion of cysts from food and water contaminated with faecal matter, or through annilingus. Inside a host, excystation occurs in the ileum, transforming cysts into trophozoites that may invade the colonic mucosal barrier.[2] Invasive amoebiasis is generally treated with metronidazole, a unique drug that is effective against luminal and tissue trophozoites.[3] Treatment failures, however, have been reported, and while the factors responsible are not clear, differences in drug susceptibility, resistance, virulence and host immune response have been implicated.[4,5]

While there are no reports of high levels of resistance to metronidazole in clinical isolates, resistance to the drug has been demonstrated *in vitro*.[6,7] In addition, resistance to the drug in other anaerobic and microaerophilic parasitic protozoa, such as *Giardia lamblia* and *Trichomonas vaginalis*, is well documented.[8,9] These findings signal forthcoming metronidazole resistance in *E. histolytica* and have spurred the search for alternative chemotherapeutic agents.

Trifluoromethionine or L-*S*-(trifluoromethyl)homocysteine is a fluorinated derivative of L-methionine. Its antimicrobial activity was first reported by Zygmunt and Tavormina[10] in 1966 when they observed that low trifluoromethionine concentrations completely inhibited microbial growth. Since then, trifluoromethionine has been shown to be effective against several pathogenic microorganisms, including *E. histolytica*, where the drug reportedly killed axenic cultures after 72 h.[11–14] It has been assumed that in these organisms trifluoromethionine is degraded by a unique enzyme called methionine γ-lyase (MGL) into α-ketobutyrate, ammonia and trifluoromethanethiol (CF_3SH). The last product is unstable under physiological conditions and breaks down to carbonothionic difluoride (CSF_2), a reactive cross-linker of primary amine groups, which is toxic to cells.[15]

Trifluoromethionine is currently being developed as an alternative chemotherapeutic agent against *E. histolytica*, but

its potential to induce resistance has not yet been demonstrated.[14] Thus, the aim of this work is to determine whether *E. histolytica* resistant to the drug can be selected *in vitro* and investigate its underlying mechanism.

Materials and methods

Chemicals and drugs

Production of trifluoromethionine was previously described.[14] Metronidazole, chloroquine, paromomycin, L-methionine, L-cysteine, trichloroacetic acid (TCA) and 3-methyl-2-benzothiazolinone hydrazone hydrochloride hydrate (MBTH) were purchased from Sigma-Aldrich (St Louis, MO, USA), while Opti-MEM medium, TRIzol reagent, SuperScript III First-Strand Synthesis System, PLUS reagent, Lipofectamine and geneticin (G418) were acquired from Invitrogen (Carlsbad, CA, USA). Tinidazole and pyridoxal 5′-phosphate (PLP) were acquired from LKT Laboratories, Inc. (St Paul, MN, USA) and Nakarai Chemicals, Ltd (Kyoto, Japan), respectively. All other chemicals were obtained from Wako Pure Chemical (Osaka, Japan) unless otherwise stated.

Parasites and cultivation

E. histolytica strain HM-1:IMSS cl6 (HM-1) and G3 strain, kindly given by David Mirelman (Weisman Institute, Israel), were cultured axenically in BI-S-33 medium for 48–72 h at 35.5°C in 13×100 mm Pyrex screw cap culture tubes or 25 cm^2 tissue culture flasks (#152094; Nunc, Roskilde, Denmark).[16]

Cultivation and generation of a trifluoromethionine-resistant E. histolytica line

Semi-confluent cultures of the HM-1 strain were exposed to 0.1 mg/L (0.5 μM) trifluoromethionine for 24 h. Spent medium and dead cells were removed by aspiration and replaced with fresh medium without the drug and cultivated until the mid-logarithmic phase. The procedure was repeated, followed by a stepwise (0.2, 0.5 or 1 mg/L) increase in drug concentration until cells growing at 4 mg/L (20 μM) trifluoromethionine were obtained, designated as the trifluoromethionine-resistant (TFMR) strain.

Cultivation of Chinese hamster ovary (CHO) cells

CHO cells were grown in Ham's F-12 medium (GIBCO, Invitrogen Co., Auckland, New Zealand) supplemented with 10% fetal calf serum (Medical Biological Laboratory International, Woburn, MA, USA) in 25 cm^2 canted-neck culture flasks (IWAKI, Tokyo, Japan) at 37°C with humidified air and 5% CO_2. For monolayer experiments, CHO cells were grown to confluency either in 24-well plates (Costar Co., Cambridge, MA, USA) or 35 mm glass-bottom culture dishes coated with collagen (MatTek Co., Ashland, MA, USA).

Growth kinetics of the TFMR strain and half maximal inhibitory concentration (IC_{50}) of trifluoromethionine and unrelated drugs

Approximately 1×10^4 cells/mL trophozoites were inoculated in 6 mL of culture medium. Cultures used for growth kinetics were maintained with or without 4 mg/L trifluoromethionine and examined every 24 h for 120 h. The number of viable cells was counted in duplicate cultures by Trypan Blue exclusion assay.[17] Briefly, cultures were incubated on ice for 10 min and 50 μL of cell suspension was transferred to a 1.5 mL tube and centrifuged at 100 **g** for 5 min at 4°C. The pellet was resuspended in 50 μL of PBS, pH 7.4, containing 2 mg/L Trypan Blue. The mixture was incubated at room temperature for 3 min and 25 μL was applied to a haemocytometer and counted.

Cultures used to determine IC_{50} were treated separately with 15 concentrations of trifluoromethionine, chloroquine, metronidazole, paromomycin and tinidazole, with a 2-fold increase between doses ranging from 0.04 mg/L to >400 mg/L. After 48 h of incubation, spent medium was aspirated and replaced with 6 mL PBS. Tubes were placed on ice for 10 min and 25 μL was applied to a haemocytometer and counted. The IC_{50} was determined by fitting a non-linear regression curve to the concentration–percentage survival growth curve. All experiments were repeated three times with two replicates per experiment.

Measurement of E. histolytica adhesion

Trophozoites in the exponential growth phase were harvested, washed with cold PBS and centrifuged at 500 **g** for 5 min at 4°C. CHO cells were trypsinized (10 mg/mL EDTA, pH 7.4, containing 5 mg/mL trypsin) in F-12 medium for 10 min, harvested by centrifugation at 500 **g** for 5 min at 4°C and washed with PBS. Amoebae and CHO cells were resuspended in Opti-MEM medium supplemented with 5 mg/mL L-cysteine and 1 mg/mL ascorbic acid. Amoebae (1×10^4 cells) and CHO cells (2×10^5 cells) were mixed in 1 mL of medium, centrifuged at 500 **g** for 5 min at 4°C and incubated on ice for up to 90 min. Following incubation, 0.8 mL of supernatant was removed and the pellet broken up by repeated rotation of the tube by hand. A drop of the cell suspension was examined as described above. All the trophozoites were examined and those with at least three CHO cells attached were considered adherent.[18] A plate adhesion assay was performed as previously described.[19] Briefly, ~1×10^5 trophozoites were seeded into a well of a 96-well plate coated with either human fibronectin (BD BioCoat Cell Environment; BD Biosciences, San Jose, CA, USA) or collagen type I (SigmaScreen; Sigma-Aldrich) and incubated under anaerobic conditions using Anaerocult A (Merck, Darmstadt, Germany) for up to 40 min at 35.5°C. The medium was removed and non-adherent cells were gently washed twice with PBS warmed to 35.5°C. Adherent cells were fixed with 40 mg/mL paraformaldehyde (TAAB Laboratories, Aldermaston, England) for 10 min and washed twice with PBS. Cells were stained with 1 mg/mL methylene blue in 100 mM borate buffer, pH 8.7, for 20 min and washed twice with distilled water. The stain was extracted with 200 μL of 20 mg/mL SDS and the absorbance measured at 660 nm using a DU 530 Spectrophotometer (Beckman Coulter, Fullerton, CA, USA).

CHO monolayer destruction assay

CHO monolayer destruction was measured as described previously with minor modifications.[20] Briefly, 1×10^6 CHO cells were seeded into 24-well plates and grown to confluency in a humidified incubator at 37°C and 5% CO_2. The medium was removed and the plates were washed with supplemented Opti-MEM medium. Approximately 2×10^5 cells of the TFMR and wild-type strains were resuspended in 2 mL supplemented Opti-MEM medium and added to each well. The plates were incubated under anaerobic conditions at 35.5°C for up to 120 min. The plates were placed on ice for 10 min to release adhered trophozoites and washed twice with cold PBS. The number of CHO cells remaining in the wells was measured as described above in the *E. histolytica* plate adhesion assay.

Substrate gel electrophoresis

Proteinase activity was detected by substrate gel electrophoresis, as described previously.[21] Briefly, 20 μg of cell lysates from the TFMR and wild-type strains were separated in a 12% (w/v) SDS–polyacrylamide

gel copolymerized with 0.1% (w/v) gelatin. The gel was incubated in 2.5% (v/v) Triton X-100 for 1 h and then in 100 mM sodium acetate, pH 4.5, 1% (v/v) Triton X-100 and 20 mM dithiothreitol (DTT) for 3 h at 37°C. The bands were visualized after staining with 0.5% (w/v) Coomassie Brilliant Blue R-250.

EhMGL activity assay

*Eh*MGL activity was measured based on the production of α-ketobutyrate, as previously described.[13] Briefly, ~2×10^7 trophozoites of the wild-type and TFMR strains were suspended in 500 μL of 100 mM sodium phosphate buffer, pH 7.0, 20 mM PLP, 0.5 mM E-64, 0.1 mM phenylmethanesulfonyl fluoride and Complete Mini-EDTA-free protease inhibitor cocktail (Roche Diagnostics, Mannheim, Germany). The suspension was subjected to three freeze–thaw cycles and insoluble materials were separated by centrifugation at 15000 **g** for 15 min at 4°C. Protein concentration was estimated with the Bio-Rad DC protein assay (Bio-Rad Laboratories, Hercules, CA, USA), with BSA as standard. The MGL reaction mixture contained 100 mM sodium phosphate buffer, pH 7.0, 20 mM PLP, 1 mM DTT, 4 mM trifluoromethionine and 1 μg/mL amoeba lysate. The reaction was initiated by adding trifluoromethionine and terminated, after 20 min incubation at 37°C, by adding 500 mg/mL TCA. The mixture was centrifuged at 15000 **g** for 10 min at 4°C and 100 μL of supernatant was incubated with 160 μL of 333 mM sodium acetate, pH 5.0 and 1.5 mM of MBTH for 60 min at 50°C. The amount of α-ketobutyrate generated was determined by measuring the absorbance at 320 nm with sodium 2-oxobutyrate (Fluka BioChemika, Buchs, Switzerland) as standard.

Immunoblot analysis

Cell lysates were prepared as described above, with all subsequent incubations performed at room temperature. Total protein (10–30 μg) was separated on a 12% (w/v) SDS–polyacrylamide gel and subsequently electrotransferred onto nitrocellulose membranes (Hybond-C Extra; Amersham Biosciences, Little Chalfont, Bucks, UK), as described previously.[13] Membranes were blocked by incubation in 5% (w/v) non-fat dried milk (BD, Le Pont de Claix, France) in TBST [50 mM Tris-HCl, pH 8.0, 150 mM NaCl and 0.05% (v/v) Tween 20] for 1.5 h. Blots were reacted with primary anti-*Eh*MGL1 or anti-*Eh*MGL2 antibody (1:1000) for 1 h.[22] The membranes were washed with TBST and further reacted with alkaline phosphatase-conjugated anti-rabbit (1:2000) for 1 h. After further washings with TBST, specific proteins were visualized with an alkaline phosphatase conjugate substrate kit (Bio-Rad) and scanned with ImageScanner (Amersham Pharmacia Biotech, Piscataway, NJ, USA). The experiments were repeated in triplicate with proteins isolated from two independent extractions.

Quantitative real-time (qRT)–PCR

Semi-confluent cultures of the wild-type and TFMR strains maintained with or without 4 mg/L trifluoromethionine were harvested as described above. Total RNA was extracted using TRIzol reagent according to the manufacturer's instructions. RNA quality was assessed with the Experion automated electrophoresis system using the Experion RNA StdSens analysis kit (Bio-Rad). RNA quantity was determined by measuring absorbance at 260 nm with a NanoDrop ND-1000 UV-Vis spectrophotometer (NanoDrop Technologies, Wilmington, DE, USA). The synthesis of cDNA was performed using the SuperScript III First-Strand Synthesis System according to the manufacturer's instructions. The cDNA synthesis was completed on a DNA Engine Peltier Thermal Cycle (Bio-Rad).

The Fast SYBR Green Master Mix (Applied Biosystems, Foster City, CA, USA) was used for qRT–PCR in accordance with the manufacturer's instructions. In addition to the *EhMGL1* and *EhMGL2* primers used in this study, a housekeeping gene, the RNA polymerase II gene (*EhRNAPII*), was used as a control (Table 1). Each PCR contained 5 μL (1:50 dilution) of cDNA and 15 μL primer mix, composed of 10 μL of 2X Fast SYBR Green Master Mix, sense and antisense primers and nuclease-free water, to bring the volume to 20 μL. qRT–PCR was performed using StepOne Plus Real-Time PCR System (Applied Biosystems) with the following cycling conditions: enzyme activation at 95°C for 20 s, followed by 40 cycles of denaturation at 95°C for 3 s and annealing/extension at 60°C for 30 s. All test samples were run in triplicate, including an RT-negative control for each sample set and a blank control consisting of nuclease-free water in place of cDNA. Quantification for each target gene was determined by the ΔΔCt method with *EhRNAPII* as the reference gene.

Table 1. Primers used to quantify *EhMGL1* and *EhMGL2* by qRT–PCR and construct the plasmids for targeted gene silencing of *EhMGL1* and *EhMGL2*

Gene	Direction	Sequence (5′-3′)
qRT–PCR		
EhMGL1	sense	GTACTTTAGCAGTTTCACTTGGATG
	antisense	CCAACAGAAATTCTAACTAATTCAGG
EhMGL2	sense	TTCCCAGGTCATAAAATTGCTATGG
	antisense	AAGTTCCAAGAGAAACAGCTAATCC
EhRNAPII	sense	GATCCAACATATCCTAAAACAACA
	antisense	TCAATTATTTTCTGACCCGTCTTC
Gene silencing		
EhAP-A	sense	AGCTCTAGACCGCGGCGGCTTGCTGCACCCTTTG
	antisense	CTCTGAGCTCGTTTAAAGGCCTCATGATTGTTTGTAAGATAG
EhMGL1	sense	AGCTAGGCCTATGACTGCTCAAGATATTACTACTAC
	antisense	GCATGAGCTCCCAATGTGTAAATAATGAAACAG
EhMGL2	sense	AGCTAGGCCTATGTCTCAATTGAAGGATTTAC
	antisense	GCATGAGCTCCACCCATATCTTTAAATCTATTTCC

Restriction sites for SacII are marked by single underlining, restriction sites for SacI are marked by double underlining, and restriction sites for StuI are marked by broken underlining.

Production of EhMGL gene-silenced strains

The vector used for targeted gene silencing was constructed by amplifying the 5′ upstream region of the *EhAP-A* gene from psAP-2, using sense and antisense *EhAP-A* primers containing restriction sites for SacI, SacII and StuI at the 5′ end (Table 1).[23] The PCR product was ligated into psAP-2 and the resulting plasmid was named psAP-2-Gunma vector. The *EhMGL1* and *EhMGL2* genes were amplified by PCR from cDNA derived from the wild-type strain using specific primers (Table 1). The PCR products and psAP-2-Gunma vector were digested with StuI and SacI, and ligated to generate the *EhMGL1* and *EhMGL2* gene-silencing plasmid. These plasmids were introduced separately into trophozoites of the G3 strain by lipofection, with minor modifications as previously described.[24] Briefly, 5×10^5 cells suspended in 5 mL supplemented Opti-MEM medium were seeded into a 12-well plate and incubated under anaerobic conditions at 35.5°C for 30 min. Following incubation, 4.5 mL of medium from each well was removed and 500 μL of liposome/plasmid mixture (5 μg of plasmid, 10 μL of PLUS reagent and 20 μL of Lipofectamine in Opti-MEM medium) was added. After 5 h of transfection, cells were harvested by placing the plate on ice for 15 min, then they were added to culture tubes with 5.5 mL of cold BI-S-33 medium and incubated at 35.5°C for 24 h. Transformants were selected by adding 2 μg/mL geneticin to the cultures and gradually increasing the drug concentration to 6 μg/mL.

Statistical analysis

Correlation coefficients were calculated using the Student's *t*-test function of the Microsoft Excel statistical package (Microsoft Corp., Redmond, WA, USA). Probability levels (P) <0.05 were considered significant. IC_{50} was calculated by non-linear regression analysis using GraphPad Prism 5 software (GraphPad Software, Inc., La Jolla, CA, USA).

Results

Establishment of the TFMR strain

Exposure of wild-type trophozoites of the HM-1 strain to drug concentrations >1 mg/L (5 μM) caused changes in cell morphology, e.g. rounding and detachment within 24 h, and eventually resulted in death after 72 h. However, when we initiated the culture with permissive concentrations, e.g. 0.1 mg/L (0.5 μM) of trifluoromethionine, and gradually increased the drug concentration over 6 months, the TFMR strain, which could be maintained at 4 mg/L (20 μM) with growth rates similar to those of the parental susceptible strain, was obtained.

Growth kinetics and IC_{50} of the TFMR strain

The TFMR strain showed comparable growth kinetics with or without 4 mg/L trifluoromethionine (Figure 1a). Its population doubling time was slightly longer than the wild-type when cultured without the drug (13.3±1.1 h and 9.6±1.4 h, respectively). As reported previously, 4 mg/L trifluoromethionine caused significant growth inhibition in the wild-type as early as 24 h and a cytolytic effect within 72 h.[13,14] The growth rate of the TFMR strain in the presence of the drug, 14.2±1.5 h, was not significantly different from those cultured without the drug ($P>0.05$).

A significantly different drug concentration versus percentage survival profile was observed between resistant and susceptible cells (Figure 1b). The IC_{50} of trifluoromethionine in the TFMR and parental strain was 197.4±20.9 and 1.3±0.2 mg/L, respectively, and its resistance index was 154 (Table 2).

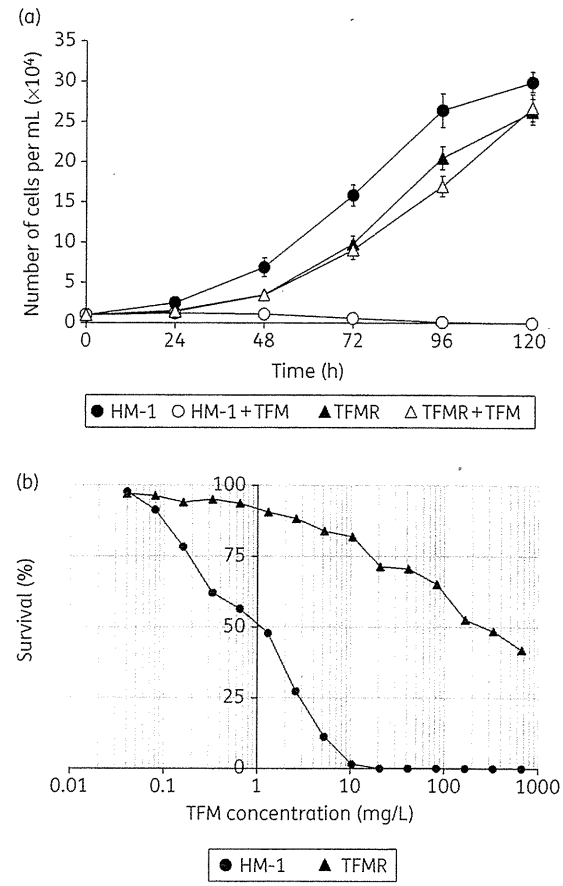

Figure 1. (a) Growth kinetics of the TFMR and wild-type strains in the presence or absence of 4 mg/L trifluoromethionine. (b) Growth inhibition by trifluoromethionine of TFMR and wild-type strains. Values shown are the means (±SEM) of at least two replicate determinations from three independent experiments. TFM, trifluoromethionine.

Trifluoromethionine resistance is irreversible upon the removal of the drug

We further maintained the TFMR strain in the presence or absence of 4 mg/L trifluoromethionine for more than 100 generations and then challenged them with 40 mg/L of the drug. The percentage survival of the TFMR strain that had been cultured without the drug, when treated with 40 mg/L trifluoromethionine, was comparable to those cultured with 4 mg/L of the drug, indicating that resistance was stable and irreversible (data not shown).

Cross-resistance

The IC_{50} and resistance indices of unrelated drugs were computed to determine whether the TFMR strain exhibited cross-resistance (Table 2). Results showed that the TFMR strain had

Table 2. IC_{50} of trifluoromethionine and drugs commonly used to treat amoebiasis against TFMR

Drug	PubChem CID no.	IC_{50} (mg/L)	Resistance index[a]
TFMR			
chloroquine	64927	8.18±4.08	0.4
metronidazole	4173	0.34±0.29	1.3
paromomycin	24176	10.70±2.96	3.1
tinidazole	5479	0.67±0.30	1.1
trifluoromethionine	165196	197.43±20.90	154.0
MGL1gs[b]			
trifluoromethionine	165196	670.09±41.78	198.7
MGL2gs[b]			
trifluoromethionine	165196	559.61±92.04	165.9

[a]Resistance index values are determined by dividing the IC_{50} of drug in TFMR by that in HM-1. No cross-resistance was observed.
[b]MGL1gs and MGL2gs refer to trophozoites transfected with *EhMGL1* and *EhMGL2* gene-silencing plasmids.

susceptibilities comparable to wild-type towards chloroquine, metronidazole, paromomycin and tinidazole. These observations indicated that the mechanisms of action and resistance of trifluoromethionine are different for these drugs.

Trifluoromethionine resistance affects cell adhesion and virulence

While 54.8±4.1% of TFMR cells adhered to three or more CHO cells, 42.2±3.6% of wild-type cells attached to three or more CHO cells ($P<0.05$; Figure 2a). The TFMR strain also showed 43.1±19.2% ($P<0.01$) or 23.5±2.8% ($P<0.05$) better attachment to fibronectin- or collagen-coated wells compared with the wild-type strain, respectively (Figure 2a). The TFMR strain, however, destroyed CHO monolayers at a slower rate, particularly at early timepoints ($P<0.05$ at 30 min; Figure 2b), indicating a slight reduction in cytopathy. This was consistent with the observed decrease in intensity of the band corresponding to *Eh*CP5, a well-established virulence determinant, in the zymogram (Figure 2c).[25,26] No gelatin degradation was observed when lysates were treated with E-64 (data not shown).

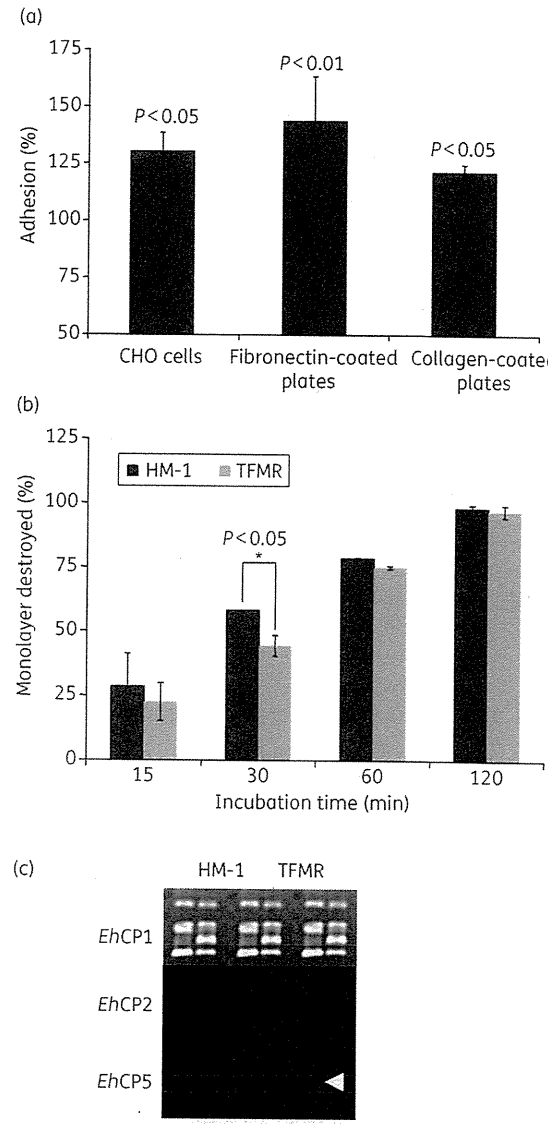

Figure 2. Effect of trifluoromethionine resistance on adhesion, cytolysis and cysteine protease secretion. (a) Effect of trifluoromethionine resistance on adhesion to CHO cells, fibronectin-coated plates or collagen-coated plates. Three assays were used to compare the adhesive capacities of the TFMR and wild-type strains. Microscopic examination of trophozoite attachment to CHO cells and colorimetric determination of cells on coated plates both show that the TFMR strain adheres more strongly compared with the parental strain. (b) Effect of trifluoromethionine resistance on cytolysis of CHO cells. The TFMR strain destroyed CHO monolayers at a slower rate, particularly at early timepoints. All experiments were repeated three times with two replicates per experiment. (c) Effect of trifluoromethionine resistance on cysteine protease secretion. Arrowhead indicates *Eh*CP5.

Repression of EhMGL in the TFMR strain

*Eh*MGL activity was not detected in the TFMR strain (Figure 3a). Repression of the enzyme was verified by western blot with anti-*Eh*MGL1 and anti-*Eh*MGL2 antibodies (Figure 3b). Analysis of mRNA steady-state level by qRT–PCR also indicated that transcription of both *EhMGL1* and *EhMGL2* were repressed (Figure 3c).

Repression of EhMGL is sufficient for trifluoromethionine resistance

These observations suggested that repression of *Eh*MGL activity alone could result in drug resistance. To answer this question, we created *EhMGL1* and *EhMGL2* gene-silenced strains. The expression of both *EhMGL1* and *EhMGL2* were abolished in the gene-silenced strains (Figure 3d). The IC_{50} value of trifluoromethionine and the resistance index of the *EhMGL1* and

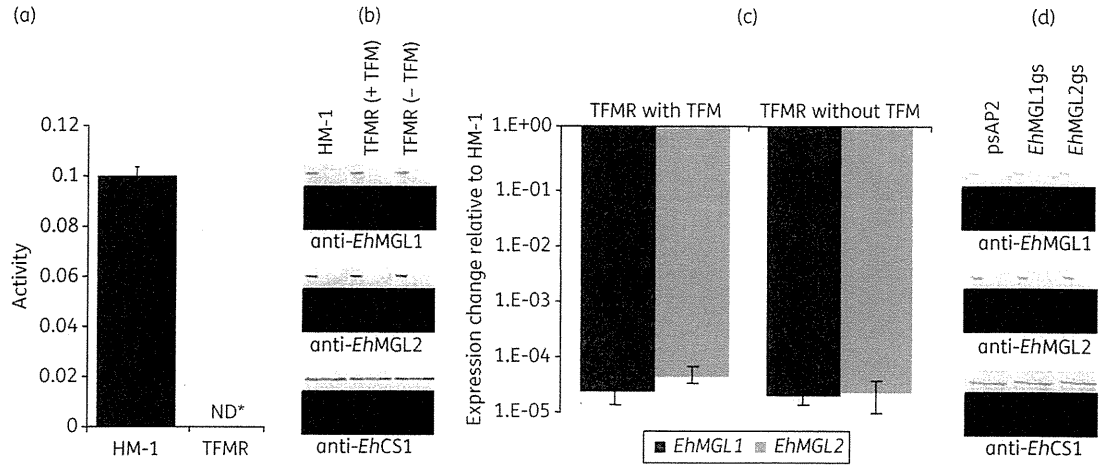

Figure 3. Repression of *Eh*MGL expression in TFMR and *EhMGL* gene-silenced strains. (a) Repression of *Eh*MGL activity in the TFMR strain. *Eh*MGL activity was measured based on the production of α-ketobutyrate (nmol/min/mg). Reactions were carried out with either 1 μg/mL lysate of the TFMR or wild-type strain and 4 mM trifluoromethionine. *Eh*MGL activity was not detected (ND) in TFMR (*$P<0.01$). (b) Repression of *Eh*MGL in TFMR cultured in the presence or absence of trifluoromethionine. (c) *EhMGL* mRNA expression ratios of the TFMR strain relative to HM-1. Quantification of each target gene was determined by the ΔΔCt method using the housekeeping gene *EhRNAPII* as a control. (d) Repression of *Eh*MGL protein in *EhMGL* gene-silenced strains was detected using methods similar to (b). All experiments were performed at least three times. TFM, trifluoromethionine.

EhMGL2 gene-silenced strains were comparable to that of the TFMR strain (Table 2).

Discussion

For more than 45 years, metronidazole has been the drug of choice to treat amoebiasis.[27] Recently, however, it has become clear that *E. histolytica* is capable of developing resistance to the drug. We previously demonstrated the potential of trifluoromethionine as an alternative chemotherapeutic agent against amoebiasis. We showed that trifluoromethionine effectively killed trophozoites *in vitro* and that a single subcutaneous or oral administration of the drug prevented the formation of amoebic liver abscess in a rodent model.[13,14] While these results demonstrate the effectiveness of the drug, its clinical application may be complicated by the parasite's capacity to develop drug resistance, which has not yet been investigated.

In principle, the evolutionary pathways of drug resistance can be reconstructed *in vitro* and, in this work, we showed that exposure of trophozoites to low levels of trifluoromethionine, followed by a gradual stepwise increase in drug concentration, leads to selection of the TFMR strain. In view of this finding, our research was directed towards the characterization of this cell line and identification of factors responsible for resistance. As shown in Figure 1(a), there was a slight delay in the growth rate of the TFMR strain compared with wild-type cells in the absence of the drug. When resistance is caused by alteration of a target, metabolic costs are expected, and this fitness loss is often reflected in reduced growth.[28,29] We next examined if the phenotype could be reversed in the absence of the drug, which is the strategy likely to be favoured by selection to avoid a permanent cost to fitness.[30] The TFMR strain, however, remained resistant to the drug after more than a year of culture in drug-free medium (data not shown). This often occurs when the target is not essential for survival or if compensatory mechanisms exist.[31,32]

Some studies have shown that cell lines resistant to one drug are often cross-resistant to closely related drugs or to unrelated compounds when they carry membrane alterations or when their mode of action is the same.[33,34] It was therefore not surprising to find that the TFMR strain was not cross-resistant to the drugs listed in Table 2. Trifluoromethionine is a fluorinated methionine analogue and its mode of action is clearly unique to microaerophilic/anaerobic microorganisms that possess MGL.[15,35]

In *E. histolytica*, differential adhesive capacity and virulence are important factors that determine the establishment and outcome of infection.[36] Studies have shown that these factors are influenced by drug resistance, and vice versa.[37,38] It is conceivable that the increased adhesion observed in the TFMR strain was necessary in selecting cells during the initial stages of drug treatment. Adhesion of cells together may create a specialized microenvironment that confers a significant advantage that promotes survival when challenged by trifluoromethionine, and could be the first step in the pathway towards resistance. Fitness loss due to acquired resistance is also reflected in decreased invasiveness.[39] The TFMR strain had slower CHO monolayer destruction, and while the reason for this phenotype is not entirely clear, it may be at least in part attributable to a decrease in the activity of cysteine proteases, particularly *Eh*CP5, which has been implicated in the parasite's cytotoxic effects on mammalian cells.[25,26] As shown in Figure 2(c), the TFMR strain had lower *Eh*CP5 levels compared with the wild-type. Since we also determined that its mRNA level was not differentially modulated (data not shown), this indicates a possible defect in enzyme processing or trafficking. Currently it is not known if the factors that determine resistance and adherence/cytopathy of the strain are genetically linked.

Previously it was shown that the amoebicidal effect of trifluoromethionine ceases when trophozoites are co-incubated with DL-propargylglycine (PPG), an inhibitor of *Eh*MGL.[13] This finding indicates that the enzyme is part of the cytotoxic mechanism of the drug and also suggests that its suppression or inactivation is a key factor in drug resistance, as shown by the phenotype of *EhMGL* gene-silenced strains toward the drug (Table 2). It is not known how this repression took place in the TFMR strain during drug treatment. However, clues were obtained from our observation that resistance was irreversible in the absence of the drug, and that this was associated with the continued repression of *EhMGL* (Figure 3b and c). It is likely that *Eh*MGL was repressed at the transcriptional level and this repression could have involved epigenetic silencing.[23] This mechanism was suggested by the high frequency of trophozoites that survived in low trifluoromethionine concentrations (data not shown). It is known that most drug-induced epigenetic repression is inherited from one generation to the next and that DNA hypermethylation constitutes one response of cells to drugs.[40,41] In *E. histolytica*, transcriptional gene silencing may also result from histone modifications that create an environment of heterochromatin around a gene that makes it inaccessible to the transcriptional machinery.[42] It is also possible that trifluoromethionine or one of its degradation products may have interfered with the binding of transcription factors to their respective cognate *cis* element, preventing the transcription of *EhMGL* genes. Epigenetic gene silencing was also suggested when we failed to restore trifluoromethionine susceptibility in the TFMR strain by episomal expression of *Eh*MGL. It was previously reported in *E. histolytica* that transcriptional silencing of the gene coding for amoebapore A resulted in the silencing of both intrinsic chromosomal and ectopically introduced episomal genes.[23] We also attempted to restore *Eh*MGL activity by the treatment of TFMR cultures with 5-azacytidine, an inhibitor of DNA methylation, but observed the continued repression of *Eh*MGL. The last observation implied that DNA methylation may not be involved in the silencing of *EhMGL*, but the possible involvement of other types of methylation remains unknown. Whether DNA hypermethylation or histone modification is responsible for *Eh*MGL repression in the TFMR strain requires further investigation, but what is clear is the non-essential role of *Eh*MGL activity for viability *in vitro*. It is possible that its absence was tolerated because of a compensatory mechanism occurring elsewhere in the genome that remains to be identified.

Suppression of enzyme activity is one mechanism that leads to drug resistance, especially if cells are not severely penalized by losing its function.[7] Initially there could have been an adaptive conflict between the development of resistance and the maintenance of sufficient *Eh*MGL activity. However, because of the specificity of trifluoromethionine to *Eh*MGL, selection took one course that resulted in complete silencing of the gene.[13] In this study we have provided evidence that in *E. histolytica*, *Eh*MGL repression is the key factor that leads to resistance to the drug.

The potential of trifluoromethionine as an amoebicide, however, remains undeniable. Its chemotherapeutic index is high and its activity is not limited to *E. histolytica*, as it is active against all microaerophilic/anaerobic organisms that possess MGL. While we showed that resistance to the drug can be induced *in vitro*, the same may not necessarily be true *in vivo*, where both drug and host factors come into play. The results presented here may provide clues on how to redesign trifluoromethionine so it is less likely to promote resistance and to help preserve its efficacy by developing appropriate therapeutic protocols.

Acknowledgements

The results of this paper were presented at the Forty-fifth Annual Japan–US Joint Conference on Parasitic Diseases, Tokyo, Japan, 2011 and at the Amebiasis Montreal 2010 Workshop: Molecular Approaches and Clinical Aspects, Montreal, Canada, 2010.

We thank Rumiko Kosugi, Ghulam Jeelani, Kumiko Nakada-Tsukui, Yumiko Saito-Nakano and other members of our laboratory for technical assistance and valuable discussions.

Funding

This work was supported by a Grant-in-Aid for Scientific Research from the Ministry of Education, Culture, Sports, Science and Technology (MEXT) of Japan (18GS0314, 18050006, 18073001, 20390119, 23390099), a grant for research on emerging and re-emerging infectious diseases from the Ministry of Health, Labour and Welfare of Japan (H20-Shinkosaiko-ippan-016, H23-Shinkosaiko-ippan-014), a grant for research to promote the development of anti-AIDS pharmaceuticals from the Japan Health Sciences Foundation (KAA1551, KHA1101) and by the Global COE Program (Global COE for Human Metabolomic Systems Biology) from MEXT, Japan.

Transparency declarations

None to declare.

References

1 Davis A, Pawlowski ZS. Amoebiasis and its control. *Bull World Health Organ* 1985; **63**: 417–26.

2 Bruckner DA. Amebiasis. *Clin Microbiol Rev* 1992; **5**: 356–69.

3 Araujo J, García M, Díaz-Suárez O *et al.* Amebiasis: relevance of its diagnosis and treatment. *Invest Clin* 2008; **49**: 265–71.

4 Pittman FE, Pittman JC. Amebic liver abscess following metronidazole therapy for amebic colitis. *Am J Trop Med* 1974; **23**: 146–50.

5 Griffin FM. Failure of metronidazole to cure hepatic amebic abscess. *N Engl J Med* 1973; **288**: 1397.

6 Wassmann C, Bruchhaus I. Superoxide dismutase reduces susceptibility to metronidazole of the pathogenic protozoan *Entamoeba histolytica* under microaerophilic but not under anaerobic conditions. *Arch Biochem Biophys* 2000; **376**: 236–8.

7 Wassmann C, Hellberg A, Tannich E *et al.* Metronidazole resistance in the protozoan parasite *Entamoeba histolytica* is associated with increased expression of iron-containing superoxide dismutase and peroxiredoxin and decreased expression of ferredoxin 1 and flavin reductase. *J Biol Chem* 1999; **274**: 26051–6.

8 Upcroft JA, Dunn LA, Wal T *et al.* Metronidazole resistance in *Trichomonas vaginalis* from highland women in Papua New Guinea. *Sex Health* 2009; **6**: 334–8.

9 Müller J, Sterk M, Hemphill A *et al.* Characterization of *Giardia lamblia* WB C6 clones resistant to nitazoxanide and to metronidazole. *J Antimicrob Chemother* 2007; **60**: 280–7.

10 Zygmunt WA, Tavormina PA. DL-*S*-Trifluoromethylhomocysteine, a novel inhibitor of microbial growth. *Can J Microbiol* 1966; **12**: 143–8.

11 Esaki N, Soda K. L-Methionine γ-lyase from *Pseudomonas putida* and *Aeromonas*. *Methods Enzymol* 1987; **143**: 459–65.

12 Coombs GH, Mottram JC. Trifluoromethionine, a prodrug designed against methionine γ-lyase-containing pathogens, has efficacy *in vitro* and *in vivo* against *Trichomonas vaginalis*. *Antimicrob Agents Chemother* 2001; **45**: 1743–5.

13 Sato D, Yamagata W, Harada S *et al.* Kinetic characterization of methionine γ-lyases from the enteric protozoan parasite *Entamoeba histolytica* against physiological substrates and trifluoromethionine, a promising lead compound against amoebiasis. *FEBS J* 2008; **275**: 548–60.

14 Sato D, Kobayashi S, Yasui H *et al.* Cytotoxic effect of amide derivatives of trifluoromethionine against the enteric protozoan parasite *Entamoeba histolytica*. *Int J Antimicrob Agents* 2010; **35**: 56–61.

15 Alston TA, Bright HJ. Conversion of trifluoromethionine to a cross-linking agent by γ-cystathionase. *Biochem Pharmacol* 1983; **32**: 947–50.

16 Diamond LS, Harlow DR, Cunnick CC. A new medium for the axenic cultivation of *Entamoeba histolytica* and other *Entamoeba*. *Trans R Soc Trop Med Hyg* 1978; **72**: 431–2.

17 Strober W. Trypan blue exclusion test of cell viability. *Curr Protoc Immunol* 2001; A.3B.1–2.

18 Petri WA Jr, Ravdin JI. Protection of gerbils from amebic liver abscess by immunization with the galactose-specific adherence lectin of *Entamoeba histolytica*. *Infect Immun* 1991; **59**: 97–101.

19 Ravdin JI, Guerrant RL. Role of adherence in cytopathogenic mechanisms of *Entamoeba histolytica*. Study with mammalian tissue culture cells and human erythrocytes. *J Clin Invest* 1981; **68**: 1305–13.

20 Hellberg A, Nickel R, Lotter H *et al.* Overexpression of cysteine proteinase 2 in *Entamoeba histolytica* or *Entamoeba dispar* increases amoeba-induced monolayer destruction *in vitro* but does not augment amoebic liver abscess formation in gerbils. *Cell Microbiol* 2001; **3**: 13–20.

21 Hellberg A, Leippe M, Bruchhaus I. Two major 'higher molecular mass proteinases' of *Entamoeba histolytica* are identified as cysteine proteinases 1 and 2. *Mol Biochem Parasitol* 2000; **105**: 305–9.

22 Tokoro M, Asai T, Kobayashi S *et al.* Identification and characterization of two isoenzymes of methionine γ-lyase from *Entamoeba histolytica*: a key enzyme of sulfur-amino acid degradation in an anaerobic parasitic protist that lacks forward and reverse trans-sulfuration pathways. *J Biol Chem* 2003; **278**: 42717–27.

23 Bracha R, Nuchamowitz Y, Mirelman D. Transcriptional silencing of an amoebapore gene in *Entamoeba histolytica*: molecular analysis and effect on pathogenicity. *Eukaryot Cell* 2003; **2**: 295–305.

24 Nakada-Tsukui K, Okada H, Mitra BN *et al.* Phosphatidylinositol-phosphates mediate cytoskeletal reorganization during phagocytosis via a unique modular protein consisting of RhoGEF/DH and FYVE domains in the parasitic protozoon *Entamoeba histolytica*. *Cell Microbiol* 2009; **11**: 1471–91.

25 Freitas MA, Fernandes HC, Calixto VC *et al.* *Entamoeba histolytica*: cysteine proteinase activity and virulence. Focus on cysteine proteinase 5 expression levels. *Exp Parasitol* 2009; **122**: 306–9.

26 Tillack M, Nowak N, Lotter H *et al.* Increased expression of the major cysteine proteinases by stable episomal transfection underlines the important role of EhCP5 for the pathogenicity of *Entamoeba histolytica*. *Mol Biochem Parasitol* 2006; **149**: 58–64.

27 Löfmark S, Edlund C, Nord CE. Metronidazole is still the drug of choice for treatment of anaerobic infections. *Clin Infect Dis* 2010; **50** Suppl 1: S16–23.

28 Alekshun MN, Levy SB. Molecular mechanisms of antibacterial multidrug resistance. *Cell* 2007; **128**: 1037–50.

29 Andersson DI. The biological cost of mutational antibiotic resistance: any practical conclusions? *Curr Opin Microbiol* 2006; **9**: 461–5.

30 Massey RC, Buckling A, Peacock SJ. Phenotypic switching of antibiotic resistance circumvents permanent costs in *Staphylococcus aureus*. *Curr Biol* 2001; **11**: 1810–4.

31 Jiang H, Patel JJ, Yi M *et al.* Genome-wide compensatory changes accompany drug-selected mutations in the *Plasmodium falciparum* crt gene. *PLoS One* 2008; **3**: e2484.

32 Ma C, Tran J, Li C *et al.* Secondary mutations correct fitness defects in *Toxoplasma gondii* with dinitroaniline resistance mutations. *Genetics* 2008; **180**: 845–56.

33 Upcroft JA, Upcroft P. Drug resistance and *Giardia*. *Parasitol Today* 1993; **9**: 187–90.

34 Bech-Hansen NT, Till JE, Ling V. Pleiotropic phenotype of colchicine-resistant CHO cells: cross-resistance and collateral sensitivity. *J Cell Physiol* 1976; **88**: 23–31.

35 Dannley RL, Taborsky RG. Synthesis of DL-*S*-trifluoromethylhomocysteine (trifluoromethylmethionine). *J Organic Chem* 1957; **22**: 1275–6.

36 Flores-Romo L, Estrada-García T, Shibayama-Salas M *et al.* *In vitro Entamoeba histolytica* adhesion to human endothelium: a comparison using two strains of different virulence. *Parasitol Res* 1997; **83**: 397–400.

37 Giha HA, Elbashir MI, A-Elbasit IE *et al.* Drug resistance-virulence relationship in *Plasmodium falciparum* causing severe malaria in an area of seasonal and unstable transmission. *Acta Trop* 2006; **97**: 181–7.

38 Landowski TH, Olashaw NE, Agrawal D *et al.* Cell adhesion-mediated drug resistance (CAM-DR) is associated with activation of NF-κB (RelB/p50) in myeloma cells. *Oncogene* 2003; **22**: 2417–21.

39 Nowak N, Lotter H, Tannich E *et al.* Resistance of *Entamoeba histolytica* to the cysteine proteinase inhibitor E64 is associated with secretion of pro-enzymes and reduced pathogenicity. *Biol Chem* 2004; **279**: 38260–6.

40 Adam M, Murali B, Glenn NO *et al.* Epigenetic inheritance based evolution of antibiotic resistance in bacteria. *BMC Evol Biol* 2008; **8**: 52.

41 Nyce J. Drug-induced DNA hypermethylation and drug resistance in human tumors. *Cancer Res* 1989; **49**: 5829–36.

42 Huguenin M, Bracha R, Chookajorn T *et al.* Epigenetic transcriptional gene silencing in *Entamoeba histolytica*: insight into histone and chromatin modifications. *Parasitology* 2010; **137**: 619–27.

OPEN ACCESS Freely available online

PLoS NEGLECTED TROPICAL DISEASES

Sulfate Activation in Mitosomes Plays an Important Role in the Proliferation of *Entamoeba histolytica*

Fumika Mi-ichi[1¤], Takashi Makiuchi[1], Atsushi Furukawa[1,2], Dan Sato[3], Tomoyoshi Nozaki[1,4]*

1 Department of Parasitology, National Institute of Infectious Diseases, Shinjuku, Tokyo, Japan, **2** Graduate School of Medicine, Gunma University, Maebashi, Gunma, Japan, **3** Institute for Advanced Biosciences, Keio University, Tsuruoka, Yamagata, Japan, **4** Graduate School of Life and Environmental Sciences, University of Tsukuba, Tsukuba, Ibaraki, Japan

Abstract

Mitochondrion-related organelles, mitosomes and hydrogenosomes, are found in a phylogenetically broad range of organisms. Their components and functions are highly diverse. We have previously shown that mitosomes of the anaerobic/microaerophilic intestinal protozoan parasite *Entamoeba histolytica* have uniquely evolved and compartmentalized a sulfate activation pathway. Although this confined metabolic pathway is the major function in *E. histolytica* mitosomes, their physiological role remains unknown. In this study, we examined the phenotypes of the parasites in which genes involved in the mitosome functions were suppressed by gene silencing, and showed that sulfate activation in mitosomes is important for sulfolipid synthesis and cell proliferation. We also demonstrated that both Cpn60 and unusual mitochondrial ADP/ATP transporter (mitochondria carrier family, MCF) are important for the mitosome functions. Immunoelectron microscopy demonstrated that the enzymes involved in sulfate activation, Cpn60, and mitochondrial carrier family were differentially distributed within the electron dense, double membrane-bounded organelles. The importance and topology of the components in *E. histolytica* mitosomes reinforce the notion that they are not "rudimentary" or "residual" mitochondria, but represent a uniquely evolved crucial organelle in *E. histolytica*.

Citation: Mi-ichi F, Makiuchi T, Furukawa A, Sato D, Nozaki T (2011) Sulfate Activation in Mitosomes Plays an Important Role in the Proliferation of *Entamoeba histolytica*. PLoS Negl Trop Dis 5(8): e1263. doi:10.1371/journal.pntd.0001263

Editor: Daniel Eichinger, New York University School of Medicine, United States of America

Received March 24, 2011; **Accepted** June 18, 2011; **Published** August 2, 2011

Funding: This work was supported by a Grant-in-Aid for Scientific Research from the Ministry of Education, Culture, Sports, Science and Technology (MEXT) of Japan to T.N. (18GS0314, 18073001, 20390119), a grant for research on emerging and re-emerging infectious diseases from the Ministry of Health, Labour and Welfare of Japan (H20-Shinkosaiko-016), and a grant for research to promote the development of anti-AIDS pharmaceuticals from the Japan Health Sciences Foundation to T.N. The funders had no role in study design, data collection and analysis, decision to publish, or preparation of the manuscript.

Competing Interests: The authors have declared that no competing interests exist.

* E-mail: nozaki@nih.go.jp

¤ Current address: Division of Molecular and Cellular Immunoscience, Department of Biomolecular Sciences, Saga University, Saga, Japan

Introduction

Mitosomes and hydrogenosomes are mitochondrion-related organelles and found in a phylogenetically broad range of eukaryotes. Since organisms that possess hydrogenosomes or mitosomes do not cluster together in eukaryote phylogenies, it is suggested that secondary losses and changes in mitochondrial functions have independently occurred multiple times in eukaryote evolution [1]. This view largely agrees to the observation that the components and functions of the mitochondrion-related organelles differ between organisms [1,2].

Entamoeba histolytica, a widespread intestinal protozoan parasite [3], possesses highly divergent mitosomes [4–6]. We have previously shown that sulfate activation is compartmentalized in *E. histolytica* mitosomes [5]. As sulfate activation generally occurs in the cytoplasm or plastids in eukaryotes [5,7], its compartmentalization to mitosomes is unprecedented. *Mastigamoeba balamuthi*, a free-living amoeba that is distantly related to *E. histolytica*, also possesses mitochondrion-related organelle. An expressed sequence tags (EST) project showed that the organism has enzymes for sulfate activation, and one of the enzymes has the putative mitochondrial targeting signal at the amino terminus (Jan Tachezy, personal communication). *Trichomonas vaginalis, Giardia intestinalis, and Cryptosporidium parvum*, which also possess mitochondrion-related organelles, i.e., hydrogenosome and mitosome, apparently lack genes encoding these enzymes. Phylogenetic analyses further revealed that *E. histolytica* appears to have acquired enzymes involved in sulfate activation from distinct prokaryotic and eukaryotic lineages by lateral gene transfer [5]. Therefore, sulfate activation is not a common function of the mitochondrion-related organelles, but may be a unique feature of a lineage *E. histolytica* and *M. balamuthi* belong to. Although iron sulfur cluster biosynthesis is shared by aerobic eukaryotes and highly divergent *G. intestinalis* mitosomes and *T. vaginalis* hydrogenosomes [8–11], it still remains to be unequivocally determined whether iron sulfur cluster biosynthesis is exclusively compartmentalized to the mitosomes in *E. histolytica* and *M. balamuthi* [12].

Sulfate is generally activated in two steps. Inorganic sulfate is converted to adenosine-5′-phosphosulfate (APS), in a reaction catalyzed by ATP sulfurylase (AS), and further converted to 3′-phosphoadenosine-5′-phosphosulfate (PAPS) in a reaction catalyzed by APS kinase (APSK). Pyrophosphate concomitantly produced in the first reaction needs to be decomposed to phosphates by inorganic pyrophosphatase (IPP). PAPS acts as a sulfuryl donor to transfer the sulfuryl moiety to various acceptors by sulfotransferases, resulting into the formation of sulfurylated macromolecules such as mucopolysaccharides, sulfolipids, and sulfoproteins [7,13,14]. Alternatively, activated sulfate (APS and

Author Summary

The mitochondrion and its related organelles are ubiquitous in all extant eukaryotic cells. The mitochondria are believed to have originated from the endosymbiosis of α-proteobacteria in an ancestral eukaryote, and show diverse structures, contents, and functions. Evolution and diversification of mitochondrion-related organelles remains one of the central themes in biology. *Entamoeba histolytica*, which causes intestinal and extraintestinal amebiasis in humans, possesses a highly divergent form of mitochondrion-related organelles, named "mitosomes." Previously, we demonstrated that sulfate activation is the major function of mitosomes in *E. histolytica*. As the sulfate activation pathway was discovered only in the cytoplasm and plastids in other eukaryotic organisms, its compartmentalization to mitosomes is unprecedented. In this study, we showed that this pathway is important for sulfolipid synthesis and cell proliferation in *E. histolytica*. Together, we infer that *E. histolytica* mitosomes are not just rudimentary or residual mitochondria, but important for proliferation of *E. histolytica*. Thus, *E. histolytica* represents a useful model to understand evolutionary constraints of mitochondrion-related organelles in eukaryotes.

PAPS) is reduced and assimilated into cysteine [13]. In addition, activated sulfate is reduced to sulfide and used as a terminal electron acceptor in the anaerobic respiration in sulfate-reducing bacteria [15]. The *E. histolytica* genome contains 10 potential genes encoding for sulfotransferases, but lacks the enzymes for sulfate reduction [5]. Consistent with this, activated sulfate is predominantly incorporated in sulfolipids in *E. histolytica* [5]. Sulfolipids are a class of lipids containing sulfur. Among them, sulfoquinovosyldiacylglycerol and sulfolipid-I were well characterized in plastids and *Mycobacterium tuberculoris*, respectively [16,17]. Sulfoquinovosyldiacylglycerol was shown to be involved in photosynthesis. Sulfolipid-I was identified as a virulence factor in *M. tuberculoris*. However, the structure and function of sulfolipids in *E. histolytica* remains largely unknown.

While the sulfate activation has been demonstrated as the major metabolic pathway in *E. histolytica* mitosomes [5], the physiological role of this mitosome-confined pathway remains unknown. In this study, we attempted to uncover the role of mitosomes in *E. histolytica* by using the parasites in which genes for the enzymes involved in sulfate activation, MCF, and Cpn60 were knocked down by gene silencing. We showed that these mitosomal proteins are indeed important for sulfolipid production and cell growth. We also demonstrated the localizations and topologies of the enzymes involved in sulfate activation, MCF, and Cpn60 in mitosomes by immunoelectron microscopy.

Materials and Methods

Gene silencing

G3 strain and psAP-2 plasmid were kindly given by David Mirelman, Weisman Institute, Israel [18]. An upstream region of *ap-a* gene was amplified from psAP-2 using 5′-AGCTCTAGACCGCGGCGGCTTGCTGCACCCTTTG-3′ (forward primer; *Sac*II site is underlined) and 5′-CTCTGAGCTCGTTTAAAGGCCT CATGATTGTTTGTAAGATAT G-3′ (reverse primer; *Sac*I, and *Stu*I sites are double-, and broken-underlined, respectively). PCR product was digested with *Sac*I and *Sac*II, and ligated into *Sac*I- and *Sac*II-double digested psAP-2 vector to produce psAP-2-Gunma. Approximately 380-450-bp fragments corresponding to the 5′ end of the open reading frame of *Cpn60, Mcf, As, Apsk,* and *Ipp* genes, respectively, were amplified by PCR using the following primers sets (*Sac*I and *Stu*I sites are single- and double-underlined, respectively):

5′-AAAGGCCTATGCTTTCATCTTCAAGTCATT-3′ (forward) and 5′-GGGGAGCTCTTTGTAATTTTCTTTAATAC-3′ (reverse) for *Cpn60*; 5′-CATCAGGCCTATGATACAAGGTATGACTTATAAACG-3′ (forward) and 5′-ACGCGAGCTCCTAGCAGTACCAAAGAATGTATC-3′ (reverse) for *Mcf*; 5′-CATCAGGCCTATGAGCATTCAAGAAAACTTAAACAAC-3′ (forward) and 5′-ACTTGAGCTCGGTCAATTTCAATAGTTCCTGAG-3′ (reverse) for *As*; 5′-GATCAGGCCTATGGCTACTGCTAAGATTGCTG-3′ (forward) and 5′-GACTGAGCTCGAGGTGGTGGTTCAACAAATTC-3′ (reverse) for *Apsk*; 5′- CATCAGGCCTATGTCAATTACTTCTATTGTCCCC-3′ (forward) and 5′-CACCGAGCTCATCAATTGGATCATTATCTCCAGG-3′ (reverse) for *Ipp*. The PCR fragments were digested with *Stu*I and *Sac*I, and ligated into the *Stu*I- and *Sac*I-double digested psAP-2-Gunma to produce the plasmids used for gene silencing. Lipofection of trophozoites and selection of transformants were performed as previously described [5].

Production of anti-EhCpn60, EhAPSK, and EhIPP antisera

The open reading frame of *Cpn60*, *Apsk*, and *Ipp* was PCR-amplified with primers containing a *Bam*HI restriction site, digested with *Bam*HI, and ligated into *Bam*HI-digested pCOLD1 to yield pCOLD1-Cpn60, pCOLD1-APSK, and pCOLD1-IPP, respectively. These constructs were introduced into *E. coli* BL21 (DE3) cells. Expression and purification of the recombinant proteins were performed as previously described [19]. Briefly, *E. coli* pellet was suspended in 20 ml of lysis buffer (50 mM Tris–HCl, pH 8.0, 300 mM NaCl, and 20 mM imidazole) containing 1% Triton X-100 (v/v), 100 μg/ml lysozyme, and 25 U/ml benzonase. After 15-min incubation at 4°C, the cells were sonicated on ice and centrifuged at 12,000×*g* for 20 min at 4°C. The supernatant was applied on 50% Ni^{2+}-NTA His-bind slurry (Qiagen, Tokyo, Japan). The recombinant protein-bound resin was washed three times with buffer A (50 mM Tris-HCl, pH 8.0, 300 mM NaCl) containing 20–50 mM of imidazole. The bound proteins were then eluted with buffer A containing 100 mM imidazole. Rabbit anti-Cpn60, APSK, and IPP antisera were custom made by Operon Biotechnologies (Tokyo, Japan).

Immunoblot analysis

Whole cell lysates of each gene-silenced strain were analyzed by SDS-polyacrylamide electrophoresis (PAGE) and immunoblot analysis as previously described [5]. The dilution of the primary antibodies was 1:1,000 for anti-Cpn60, anti-APSK, and anti-IPP antiserum, and 1:100 for anti-CP5 antiserum [5].

Quantitative real-time PCR (qRT-PCR)

The Fast SYBR® Green Master Mix (AB Applied Biosystems, Foster City, CA, USA) was used for qRT-PCR. RNA polymerase II gene (*Rnapol*) was used as a house-keeping reference gene. Total RNA was extracted using TRIzol® reagent (Invitrogen, Carlsbad, CA, USA). The synthesis of cDNA was performed using the SuperScript III First-Strand Synthesis System (Invitrogen). qRT-PCR was performed using the following primers: 5′-CCTATGAAAATCGATTGGACATTCTATTGCC-3′ (forward) and 5′-GCATCACCAGTAGCAAACTTTGTAACTTG-3′ (reverse) for *As*; 5′-GCCCCAATTGCACCATATCGTGAAATTAG-3′ (for-

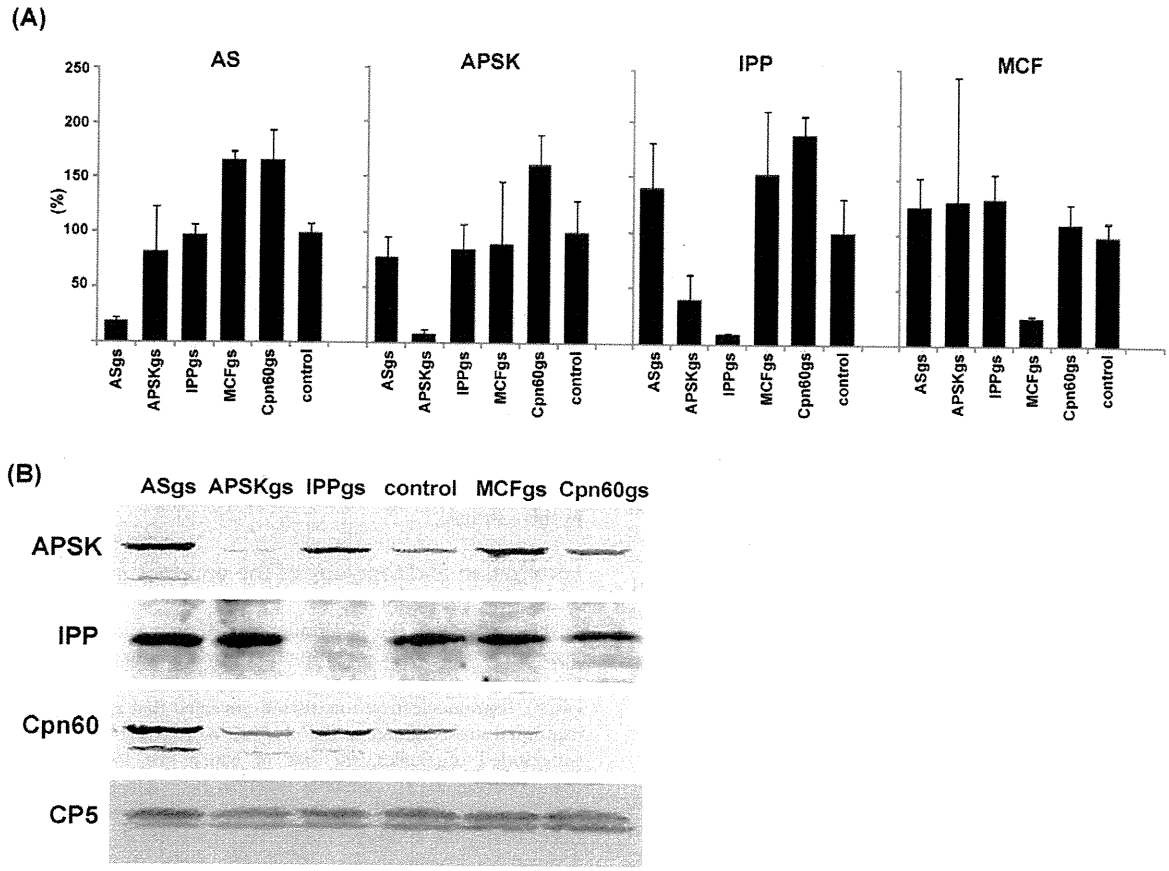

Figure 1. Gene silencing of AS, APSK, IPP, MCF, and Cpn60. (A) qRT-PCR analysis of AS, APSK, IPP, MCF expression in the gene-silenced strains. The relative expression level is expressed in percentage of the control strain. (B) Immunoblot analysis of the gene-silenced strains. Approximately 40 μg of lysates of the gene-silenced strains were subjected to SDS-PAGE and immunoblot analysis using anti-APSK, IPP, Cpn60, and CP5 antisera. Control, G3 strain transfected with an empty vector (psAP-2-Gunma).
doi:10.1371/journal.pntd.0001263.g001

ward) and 5′-GCACATTGATCAACAGACTTACCAGCAG-3′ (reverse) for *Apsk*; 5′-GATCCTCTTGCTCAAAACCATTACATCTG-3′ (forward) and 5′-GTCTAACGCCAATTTTGATAACTTCTTTTGAG-3′ (reverse) for *Ipp*; 5′-GCATGTTTTGATTTTGTTGCTCCATTAGTTCC-3′ (forward) and 5′-CACTGACTAATGGAACAACTTTGACAAATCC-3′ (reverse) for *Mcf*; 5′-GATCCAACATATCCTAAAACAACA-3′ (forward) and 5′-TCAATTATTTTCTGACCCGTCTTC-3′ (reverse) for *Rnapol*. qRT-PCR was performed using StepOne Plus Real-Time PCR System (AB Applied Biosystems) with the following cycling conditions: 95°C for 20 s, followed by 40 cycles of 95°C for 3 s, and 60°C for 30 s. All reactions were run in quadruplicate, including reverse transcriptase-minus and cDNA-minus controls. Quantification for each target gene was determined by the ΔCt method with *Rnapol* as reference gene.

Metabolic labeling

Metabolic labeling was performed as previously described [5] with some modifications. Briefly, approximately 3×10^5 trophozoites were labeled with [^{35}S]-labeled sulfate (25 mCi/mmol) in 1 mL of the BI-S-33 medium either continuously for 2, 4, or 8 h, or labeled for 4 h and chased for 4 or 24 h after removing [^{35}S]-labeled sulfate. Cells were collected and lipids were extracted with 0.5 mL of methanol and separated on a silica high-performance thin-layer chromatography plate in 35:65:8 (vol/vol/vol) methanol/chloroform/28% (w/w) ammonium hydroxide [20]. Thin-layer chromatography plates were dried and analyzed by autoradiography.

Immunoelectron microscopy analysis

E. histolytica transformants expressing epitope-tagged mitosomal proteins were previously established [5]. Approximately 5×10^5 trophozoites were resuspended in 2 ml BI-S-33 medium and seeded onto a molybdenum disk (Nissin EM Co., JAPAN) in a well of a 24-well plate. After 15-min incubation at 35.5°C, the molybdenum disk that amoebas adhered to was removed and immediately immersed in liquid propane at −175°C. The disk was further fixed and sectioned as previously described [21]. The disk was reacted with primary antibody diluted at 1:2000 (anti-Cpn60 antiserum) and 1:500 (anti-HA monoclonal antibody) in phosphate-buffered saline containing 1.5% bovine serum albumin for overnight at 4°C. The samples were then reacted with colloidal gold-conjugated anti-rabbit or anti-mouse secondary antibody (1:20) for 1 h at room temperature. Samples were examined by electron microscopy at Tokaii Microscopy., Inc (Nagoya, JAPAN).

Results

Establishment of gene-silenced strains

To investigate the role of the mitosomes and, more specifically, mitosome-localized sulfate activation pathway, chaperones, and ADP/ATP transporter, we established the *E. histolytica* strains in which AS, APSK, IPP, MCF, and Cpn60 genes were knocked down by gene silencing [18,22]. These gene-silenced strains were designated ASgs, APSKgs, IPPgs, MCFgs, and Cpn60gs strains, respectively. AS, APSK, and IPP are essential components of the sulfate activation pathway, while MCF transports ADP/ATP across the mitosomal membrane and Cpn60 functions as a mitosome-specific chaperone [5]. Reduction of gene expression of each target gene was verified by qRT-PCR in the gene-silenced strains. The amount of the steady-state transcript of the genes involved in sulfate reduction was reduced by 80.4–91.8% (Figure 1A). The changes of the level of the transcripts of irrelevant genes ranged 0.4–1.8 fold of the control, but mostly varied only in the range of 0.8–1.6 fold. In APSKgs, IPPgs, and Cpn60gs strains, the reduction of each target protein was confirmed by immunoblotting (Figure 1B). Although we observed slight variations in the amount of APSK and Cpn60 in the gene-silenced strains (e.g., reduction of Cpn60 protein in MCFgs strain), these variations did not correlate with the changes in the transcripts. In APSKgs strain, IPP mRNA level was also slightly decreased, while its protein level remained unchanged.

Effects of repression of sulfate activation on sulfolipid synthesis

We previously showed that in *E. histolytica* trophozoites, the majority of activated sulfate are incorporated into sulfolipids [5]. So, we first examined the time course of accumulation of sulfolipids in ASgs, APSKgs, IPPgs, and control mock transformants (G3 strain transfected with an empty vector), by metabolic labeling. As shown in Figure 2A, in the control mock transformant, four major groups of sulfolipids (I-IV) were detected by thin layer chromatography, similar to HM1 reference strain as described previously [5]. The amount of sulfolipids (I–IV) changed differently in the individual gene-silenced strains. However, the trend of the decrease of each sulfolipid was similar among the strains: II and III were highly affected, whereas I and IV were not affected as muh as II and III. Thus, only the total count of labeled sulfated lipids is shown. At 8 h of continuous labeling with [^{35}S]-sulfate, the sulfate activation activity in ASgs, APSKgs, and IPPgs was decreased to 54.1±11.0, 49.1±15.9, and 24.0±0.6%, respectively, as compared to the control (Figure 2B). We also examined the stability of the accumulated products by pulse-chase experiment. The degradation kinetics of all transformants was similar (Figure 2C). These results indicate that AS, APSK, and IPP are indeed involved in sulfate activation.

We next examined the growth of the gene-silenced strains. Although ASgs, APSKgs, IPPgs, and the mock control showed similar growth pattern, the three former strains showed marked growth retardation. The doubling time of ASgs, APSKgs, and IPPgs was 24.9±2.7, 26.1±2.0, and 34.4±1.2 h, respectively, while that of the control was 15.0±0.8 h (Figure 2D). The degree of the growth inhibition was parallel to the level of repressed sulfate activation activity (Figure 2B, growth rate: IPPgs<APSKgs = ASgs<control). These results indicate that sulfate activation is important for cell proliferation.

Chlorate (ClO_3^-), a known inhibitor for AS in mammals and fungi [23–25], inhibited cell growth of *E. histolytica* (IC_{50} = 10.5 mM). At this concentration, the sulfate activation activity (as expressed as the total count of labeled sulfated lipids) was decreased to 22.5% of the control. Furthermore, the apparent IC_{50} of the recombinant *E. histolytica* AS by chlorate was determined to be 3.55±0.25 mM. These results support the premise that sulfate activation plays an important role for proliferation.

Effects of repression of Cpn60 and MCF on sulfolipid production and growth

We also investigated the role of Cpn60 and MCF in sulfate activation. In Cpn60gs and MCFgs strains, the activity of sulfate activation was decreased to 20.2±5.4 and 34.2±1.1%, respectively, as compared to the control (Figure 2B). MCFgs and Cpn60gs strains also showed marked growth defect; the doubling time of MCFgs and Cpn60gs strains was 41.7±5.5 and 82.4±14.5 h, respectively (Figure 2D). These results indicate that MCF and Cpn60 significantly contribute to sulfolipid synthesis and cell proliferation. However, as growth of these gene-silenced strains was moderately-to-severely affected, the growth retardation should be taken into account for the impaired sulfolipid synthesis in these strains.

Localization and topology of the enzymes in sulfate activation pathway

We investigated the localization and topology of the proteins involved in sulfate activation pathway by exploiting the transformants expressing the HA-tagged proteins (AS, APSK, IPP, and MCF). Immunoelectron microscopy revealed that all the proteins examined are confined to the electron dense double-membrane-surrounded organelles, the size of which are 150–400 nm in diameter (Figure 3A). Double labeling with anti-HA and anti-Cpn60 antibodies showed that these proteins were co-localized with Cpn60, the authentic marker of mitosomes (Figure 3B; only AS and MCF were shown). While AS, APSK, IPP, and Cpn60 were evenly distributed throughout the luminal (matrix) part of mitosomes, MCF was concentrated on the inner membrane of mitosomes. The quantification results for the distribution of AS, APSK, IPP, MCF, and Cpn60 were summarized in Table 1. These proteins were found to be 140-560-fold concentrated in mitosomes as compared to the cytosol. The number of mitosomes was estimated to be 32.1±9.7 per section (10 sections of 10 cells were examined). We estimated by the method described previously [12] that the mitosomes density is about 1.57 per μm^3, the number of mitosomes per trophozoite is about 6585, and the volume percentage of mitosomes is about 1.2%, in the *E. histolytica* transformant lines used in this study.

Discussion

In our previous report, we showed that mitosomes of *E. histolytica* uniquely possess sulfate activation pathway, while they have lost most of the functions shared by other aerobic eukaryote mitochondria including TCA cycle, electron transport, oxidative phosphorylation, and β-oxidation of fatty acids [5]. Only three chaperones and two mitochondrial-type transporters aside from the components in the sulfate activation pathway are retained in *E. histolytica* mitosomes [4,5,26]. Since the sulfate activation pathway is not typically confined to the mitochondria, and generally present in either the cytosol or plastid in eukaryotes [5,7], the physiological significance of its compartmentalization in *E. histolytica* remains unknown [5].

In this report, we have provided several lines of direct and indirect biochemical and cell biological evidence that the sulfate activation pathway plays an important role in the production of sulfolipids and the growth of trophozoites. Consistent with this

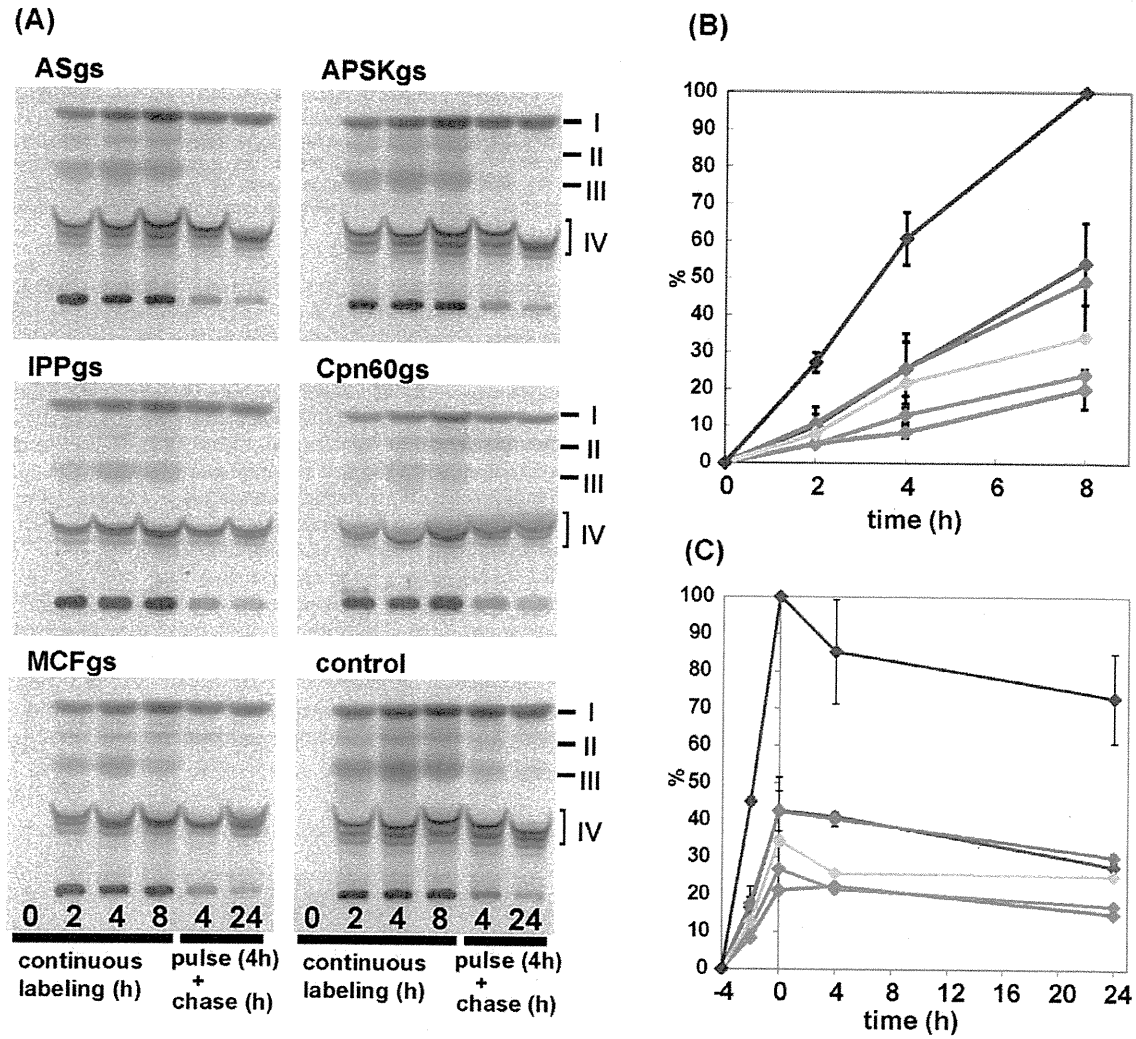
(A)
ASgs
APSKgs
IPPgs
Cpn60gs
MCFgs
control
I
II
III
IV
0 2 4 8 4 24
continuous labeling (h)
pulse (4h) + chase (h)
(B)
%
time (h)
(C)
%
time (h)
(D)
cell density (/ml)
time (h)
ASgs
APSKgs
IPPgs
Cpn60gs
MCFgs
control

Figure 2. Repression of sulfate activation in the gene-silenced strains. (A) Thin layer chromatography of the extract from the gene-silenced strains. The trophozoites were either continuously cultured in the medium containing ^{35}S-labeled sulfate for 0–8 h (4 left lanes), or cultured with ^{35}S-sulfate for 4 h and subsequently cultured in the isotope-free medium for 4 or 24 h (2 right lanes). Four major groups of sulfolipids are labeled ("I–IV"). (B–C) Quantitation of total sulfolipid synthesis. The kinetics of the total count of ^{35}S incorporated into the sulfated polar lipids that were separated by thin layer chromatography, and measured by densitometric analysis using an image analyzer (Fuji), are shown. The trophozoites were either continuously cultured in the medium containing ^{35}S-labeled sulfate for 8 h (B), or cultured with ^{35}S-sulfate for 4 h and subsequently cultured in the isotope-free medium for 24 h (C). The level of incorporated ^{35}S-sulfate at each point was normalized with protein concentrations and expressed as relative values to the level of ^{35}S incorporated in the control strain at 8 h (in continuous labeling experiments, B) or at 0 h (in pulse-chase experiments, C) as 100%. (D) Growth kinetics of the gene-silenced strains. Control; G3 strain transfected with the empty vector (psAP-2-Gunma).
doi:10.1371/journal.pntd.0001263.g002

premise, the AS inhibitor, chlorate, inhibited the sulfolipid production in and the growth of *E. histolytica*. Further supporting the specificity of chlorate to AS, two amino acid residues (Asn198 and His201) of *Saccharomyces cerevisiae* AS, which were implicated in the chlorate binding [24], as well as Arg362, which is located in the highly conserved ISGTxxR motif, are well conserved in *E. histolytica* AS (Asn211, His214, and Arg375).

In addition to the importance of the enzymes in the sulfate activation pathway, we demonstrated that MCF, and Cpn60 also play an important role in cell proliferation. The phenotype of Cpn60gs is most likely attributable to multiple defects as Cpn60 is required for the folding and quality control of mitosome-targeted proteins [27]. Lack of Cpn60 should result in an inability to fold freshly-imported mitosomal proteins and therefore make them functional. This notion likely explains why the knockdown of Cpn60 impaired the cell growth more severely than that of the genes directly involved in sulfate activation. The phenotype of MCFgs strain was probably accounted for the lack of ATP supply required for chaperone functions and for the activation of inorganic sulfate into PAPS in AS- and APSK-catalyzed reactions. The latter possibility was supported by the observation that in MCFgs strain, the activity of sulfate activation was significantly reduced while the amount of the proteins involved in the pathway was not changed. Lack of MCF would impair the ADP/ATP ratio in mitosomes, and, as Cpn60 needs ATP to function, likely cause a similar effect as Cpn60gs. We assume that MCF and Cpn60 are not indispensable for sulfolipid synthesis per se, but gene silencing of these house-keeping proteins resulted in broader effects, and thus severe impairment of mitosome functions.

Immunoelectron microscopy revealed that MCF is mainly localized on the inner mitosome membrane. Although membrane topology may need to be further verified, the observed localization of MCF agrees well with its biochemical characteristics, previously demonstrated: ATP import and ADP export [28]. Recently, *E. histolytica* phosphate transporter (EhPiC) has been identified and proposed to transport phosphate released from ATP through

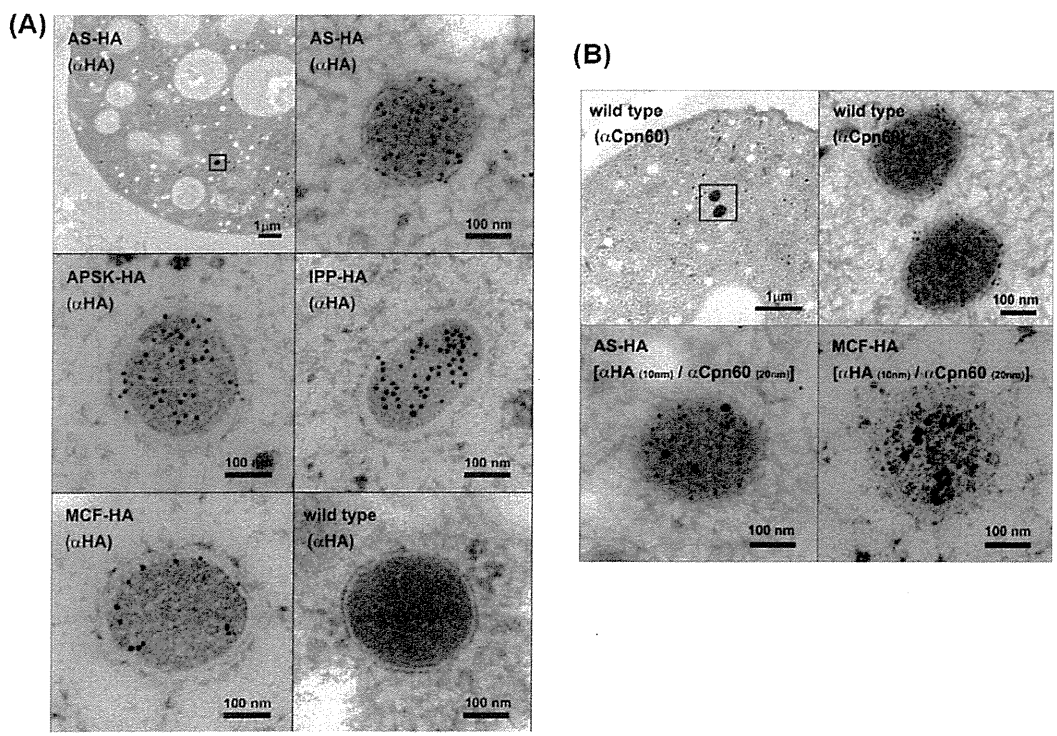

Figure 3. Localization of mitosomal proteins by immunoelectron microscopy. (A) Single labeling of AS, APSK, IPP, and MCF in the transformants that express HA-tagged proteins. Low magnification image is also shown for AS. No labeling was observed in the untransfected cells ("wild type"). (B) Co-localization of AS and MCF with Cpn60. Single staining of Cpn60 (upper panels) and double-labeling of AS and Cpn60 (bottom, left) and MCF and Cpn60 (bottom, right) labeled with colloidal gold particles of different sizes in the transformants expressing HA-tagged AS and MCF.
doi:10.1371/journal.pntd.0001263.g003

Table 1. Distribution and density of the mitosomal proteins.

		Mitosomal proteins				
Parameter		**Cpn60**	**AS**	**APSK**	**IPP**	**MCF**
Labeling density (golds μm^{-2})	Cytosol	2.13±1.15	2.86±2.12	0.930±0.900	0.908±0.744	0.950±0.908
	Mitosomes	372±102	753±151	356±101	509±197	133±95.6
Distribution ratio (mitosome cytosol^{-1})		175	263	383	561	140

The labeling density of gold particles per μm^2 area was calculated by examining eight representative sections.
doi:10.1371/journal.pntd.0001263.t001

hydrolysis by chaperones, *i.e.*, Cpn60 and mitochondrial HSP70 [26]. It is conceivable that EhPiC transports phosphate generated by IPP in sulfate activation pathway in mitosomes.

While the structure of *E. histolytica* mitosomes revealed by immunoelectron microscopy was far different from the typical eukaryotic mitochondria, it was somehow similar to the mitochondrion-related organelles, described as densely-stained double membrane-bound organelles lacking the typical cristae, in *M. balamuthi,* in shape, apparent size, number per cell, and structure [29]. Together with the fact that *M. balamuthi* possesses genes involved in sulfate activation, it is possible that sulfate activation is a unique feature shared only by *E. histolytica* and *M. balamuthi.*

The number and structure of mitosomes demonstrated in this study was slightly different from previous reports [12,30]. This may be due to the heterogeneity of mitosomes in the cells. We have also previously shown that the distribution of AS, APSK, IPP, MCF, and Cpn60 in mitosomes was not uniform [5], suggesting the heterogeneity of mitosomes in *E. histolytica.*

Acknowledgments

We thank Kumiko Nakada-Tsukui, Mohammad Abu Yousuf, Afzal Husain, and Ghulam Jeelani for technical assistance and valuable discussions. We thank Kumiko Tsuboi-Shibata and Kyoko Masuda for technical assistance. We thank David Mirelman, Weisman Institute, Israel, for G3 strain and psAP-2 plasmid.

Author Contributions

Conceived and designed the experiments: FM TM AF DS TN. Performed the experiments: FM AF. Analyzed the data: FM TM TN. Contributed reagents/materials/analysis tools: FM TM AF DS TN. Wrote the paper: FM TN.

References

1. van der Giezen M (2009) Hydrogenosomes and mitosomes: conservation and evolution of functions. J Eukaryot Microbiol 56: 221–231.
2. Keeling PJ (2007) Genomics. Deep questions in the tree of life. Science 317: 1875–6.
3. World Health Organization. (1998) The world health report 1998: life in the21st century—a vision for all. Geneva: World Health Organization Press.
4. Aguilera P, Barry T, Tovar J (2008) *Entamoeba histolytica* mitosomes: organelles in search of a function. Exp Parasitol 118: 10–16.
5. Mi-ichi F, Abu Yousuf M, Nakada-Tsukui K, Nozaki T (2009) Mitosomes in *Entamoeba histolytica* contain a sulfate activation pathway. Proc Natl Acad Sci U S A 106: 21731–21736.
6. Yousuf MA, Mi-ichi F, Nakada-Tsukui K, Nozaki T (2010) Localization and targeting of an unusual pyridine nucleotide transhydrogenase in *Entamoeba histolytica.* Eukaryot Cell 9: 926–33.
7. Patron NJ, Durnford DG, Kopriva S (2008) Sulfate assimilation in eukaryotes: fusions, relocations and lateral transfers. BMC Evol Biol 8: 39.
8. Tachezy J, Sánchez LB, Müller M (2001) Mitochondrial type iron-sulfur cluster assembly in the amitochondriate eukaryotes *Trichomonas vaginalis* and *Giardia intestinalis,* as indicated by the phylogeny of IscS. Mol Biol Evol 18: 1919–1928.
9. Tovar J, León-Avila G, Sánchez LB, Sutak R, Tachezy J, et al. (2003) Mitochondrial remnant organelles of *Giardia* function in iron-sulphur protein maturation. Nature 426: 172–176.
10. Lill R, Mühlenhoff U (2008) Maturation of iron-sulfur proteins in eukaryotes: mechanisms, connected processes, and diseases. Annu Rev Biochem77: 669–700.
11. Bandyopadhyay S, Chandramouli K, Johnson MK (2008) Iron-sulfur cluster biosynthesis. Biochem Soc Trans 36: 1112–1119.
12. Maralikova B, Ali V, Nakada-Tsukui K, Nozaki T, van der Giezen M, et al. (2010) Bacterial-type oxygen detoxification and iron-sulfur cluster assembly in amoebal relict mitochondria. Cell Microbiol 12: 331–342.
13. Strott CA (2002) Sulfonation and molecular action. Endocr Rev 23: 703–732.
14. Bradley ME, Rest JS, Li WH, Schwartz NB (2009) Sulfate activation enzymes: phylogeny and association with pyrophosphatase. J Mol Evol 68: 1–13.
15. Traore AS, Hatchikian CE, Belaich JP, Le Gall J (1981) Microcalorimetric studies of the growth of sulfate-reducing bacteria: energetics of *Desulfovibrio vulgaris* growth. J Bacteriol 145: 191–199.
16. Frentzen M (2004) Phosphatidylglycerol and sulfoquinovosyldiacylglycerol: anionic membrane lipids and phosphate regulation. Curr Opin Plant Biol 7: 270–276.
17. Schelle MW, Bertozzi CR (2006) Sulfate metabolism in mycobacteria. Chembiochem 7: 1516–1524.
18. Bracha R, Nuchamowitz Y, Anbar M, Mirelman D (2006) Transcriptional silencing of multiple genes in trophozoites of *Entamoeba histolytica.* PLoS Pathog 2: e48.
19. Jeelani G, Husain A, Sato D, Ali V, Suematsu M, et al. (2010) Two atypical L-cysteine-regulated NADPH-dependent oxidoreductases involved in redox maintenance, L-cystine and iron reduction, and metronidazole activation in the enteric protozoan *Entamoeba histolytica.* J Biol Chem 285: 26889–26899.
20. Touchstone JC (1995) Thin-layer chromatographic procedures for lipid separation. J Chromatogr B Biomed Appl 671: 169–95.
21. Baba M (2008) Electron Microscopy in Yeast. Methods Enzymol 451: 133–49.
22. Anbar M, Bracha R, Nuchamowitz Y, Li Y, Florentin A, et al. (2005) Involvement of a short interspersed element in epigenetic transcriptional silencing of the amoebapore gene in *Entamoeba histolytica.* Eukaryot Cell 4: 1775–1784.
23. Farley JR, Nakayama G, Cryns D, Segel IH (1978) Adenosine triphosphate sulfurylase from *Penicillium chrysogenum* equilibrium binding, substrate hydrolysis, and isotope exchange studies. Arch Biochem Biophys 185: 376–390.
24. Ullrich TC, Huber R (2001) The complex structures of ATP sulfurylase with thiosulfate, ADP and chlorate reveal new insights in inhibitory effects and the catalytic cycle. J Mol Biol 313: 1117–1125.
25. Baeuerle PA, Huttner WB (1986) Chlorate–a potent inhibitor of protein sulfation in intact cells. Biochem Biophys Res Commun 141: 870–877.
26. Dolezal P, Dagley MJ, Kono M, Wolynec P, Likic VA, et al. (2010) The essentials of protein import in the degenerate mitochondrion of *Entamoeba histolytica.* PLoS Pathog 6: e1000812.
27. Hood DA, Adhihetty PJ, Colavecchia M, Gordon JW, Irrcher I, et al. (2003) Mitochondrial biogenesis and the role of the protein import pathway. Med Sci Sports Exerc 35: 86–94.
28. Chan KW, Slotboom DJ, Cox S, Embley TM, Fabre O, et al. (2005) A novel ADP/ATP transporter in the mitosome of the microaerophilic human parasite *Entamoeba histolytica.* Curr Biol 15: 737–742.
29. Gill EE, Diaz-Trivino S, Barbera MJ, Silberman JD, Stechmann A, et al. (2007) Novel mitochondrion-related organelles in the anaerobic amoeba *Mastigamoeba balamuthi.* Mol Microbiol 66: 1306–1320.
30. van der Giezen M, Tovar J (2005) Degenerate mitochondria. EMBO Rep 6: 525–530.

OPEN ACCESS Freely available online

PLoS NEGLECTED TROPICAL DISEASES

Amebiasis in HIV-1-Infected Japanese Men: Clinical Features and Response to Therapy

Koji Watanabe[1,2], Hiroyuki Gatanaga[1,2]*, Aleyla Escueta-de Cadiz[3], Junko Tanuma[1], Tomoyoshi Nozaki[3], Shinichi Oka[1,2]

1 AIDS Clinical Center, National Center for Global Health and Medicine, Tokyo, Japan, **2** Center for AIDS Research, Kumamoto University, Kumamoto, Japan, **3** Department of Parasitology, National Institute of Infectious Diseases, Tokyo, Japan

Abstract

Invasive amebic diseases caused by *Entamoeba histolytica* are increasing among men who have sex with men and co-infection of ameba and HIV-1 is an emerging problem in developed East Asian countries. To characterize the clinical and epidemiological features of invasive amebiasis in HIV-1 patients, the medical records of 170 co-infected cases were analyzed retrospectively, and *E. histolytica* genotype was assayed in 14 cases. In this series of HIV-1-infected patients, clinical presentation of invasive amebiasis was similar to that described in the normal host. High fever, leukocytosis and high CRP were associated with extraluminal amebic diseases. Two cases died from amebic colitis (resulting in intestinal perforation in one and gastrointestinal bleeding in one), and three cases died from causes unrelated to amebiasis. Treatment with metronidazole or tinidazole was successful in the other 165 cases. Luminal treatment was provided to 83 patients following metronidazole or tinidazole treatment. However, amebiasis recurred in 6 of these, a frequency similar to that seen in patients who did not receive luminal treatment. Recurrence was more frequent in HCV-antibody positive individuals and those who acquired syphilis during the follow-up period. Various genotypes of *E. histolytica* were identified in 14 patients but there was no correlation between genotype and clinical features. The outcome of metronidazole and tinidazole treatment of uncomplicated amebiasis was excellent even in HIV-1-infected individuals. Luminal treatment following metronidazole or tinidazole treatment does not reduce recurrence of amebiasis in high risk populations probably due to amebic re-infection.

Citation: Watanabe K, Gatanaga H, Cadiz AE-d, Tanuma J, Nozaki T, et al. (2011) Amebiasis in HIV-1-Infected Japanese Men: Clinical Features and Response to Therapy. PLoS Negl Trop Dis 5(9): e1318. doi:10.1371/journal.pntd.0001318

Editor: Judd L. Walson, University of Washington, United States of America

Received May 10, 2011; **Accepted** August 1, 2011; **Published** September 13, 2011

Funding: This study was supported by a grant from the National Center for Global Health and Medicine. The funder had no role in study design, data collection and analysis, decision to publish, or preparation of the manuscript.

Competing Interests: The authors have declared that no competing interests exist.

* E-mail: higatana@acc.ncgm.go.jp

Introduction

Invasive amebiasis (IA) caused by *Entamoeba histolytica* is the second most common cause of mortality associated with parasitic infections worldwide, accounting for 40,000 to 100,000 deaths annually [1]. Amebiasis is transmitted by ingestion of food or water containing the cyst form of *E. histolytica*, which is prevalent in developing countries in Central and South America, Asia, and Africa. In the developed countries, most cases arise in travelers and immigrants from such endemic areas [2]. Recently, however, three developed East Asian countries (Japan, Taiwan, and South Korea) reported increased risk for amebiasis among men who have sex with men (MSM) due to oral-anal sexual contact [3–12]. The annual incidence of human immunodeficiency virus type 1 (HIV-1) infection is also increasing among MSM in these countries [13-17], resulting in growing concern on IA in HIV-1-infected MSM [6,9–12,18]. The recommended treatment for IA is metronidazole (750 mg t. i. d. for 10 days) or tinidazole (2 g q. d. for 3 days), followed by a luminal agent (paromomycin 500 mg t. i. d. for 10 days or diloxanide furoate 500 mg t. i. d. for 10 days) to eliminate intestinal colonization [18,19]. A previous report described no difference in the response to metronidazole or tinidazole treatment between HIV-1-positive and –negative IA patients [20]. However, the efficacy of luminal treatment in preventing recurrence, which can arise by relapse or re-infection, has not yet been assessed rigorously. In this study, we retrospectively analyzed 170 HIV-1-infected Japanese patients with IA, together with genomic typing of *E. histolytica* in 14 of these patients, and delineated the clinical features of IA in HIV-1-infected individuals and the efficacy of metronidazole, tinidazole and luminal treatment.

Methods

Ethics statement

The Institutional Review Board of National Center for Global Health and Medicine (Tokyo, Japan) approved this study. All patients who provided clinical samples for genotyping of *E. histolytica* gave written informed consent.

Case review

The medical records of HIV-1-infected cases diagnosed with IA at the AIDS Clinical Center, National Center for Global Health and Medicine, between April 1997 and March 2010, were reviewed. The diagnosis of IA was made when one of the following criteria was satisfied; 1) identification of and/or positive PCR (methods; see below) in clinical specimens (stool or punctuate-exudate) for erythrophagocytic trophozoites in patients with IA-

Author Summary

Amebiasis is usually transmitted by ingestion of contaminated food or water in developing countries. Recently, however, increased risk for amebiasis among men who have sex with men (MSM) due to oral-anal sexual contact was reported in developed countries, resulting in growing concern on amebiasis in HIV-1-infected MSM. The recommended treatment of amebiasis is metronidazole or tinidazole, followed by a luminal agent to eliminate intestinal cyst colonization. However, the efficacy of luminal treatment in preventing recurrence has not been assessed yet. In this study, we analyzed the medical records of 170 patients with amebiasis and HIV-1 co-infection. Treatment with metronidazole or tinidazole was excellent whereas luminal treatment did not reduce the frequency of recurrence of amebiasis. Recurrence was more frequent in those MSM with signs of sexual activity such as syphilis infection. Luminal treatment following metronidazole or tinidazole treatment does not reduce recurrence of amebiasis in high risk populations.

related symptoms, e.g., fever and liver abscess, or tenesmus and diarrhea, 2) high serum titer (>1:100) for antibody against *E. histolytica* in patients with IA-related symptoms in whom microbiological cultures or histological examination of clinical specimens did not identify any pathogen, and who showed improvement of IA symptoms following metronidazole or tinidazole monotherapy [10–12]. The medical records were surveyed for patients' characteristics, presenting forms of clinical IA [e.g., colitis, amebic liver abscess (ALA), and perianal abscess], HIV-1-induced immunocompromised status, and symptoms, laboratory data and serological markers of other sexually-transmitted diseases (STD) including syphilis, hepatitis B and C viruses (HBV and HCV). After completion of treatment for IA, the medical records were followed-up until March 2010, excluding those cases found to have died or lost to follow-up.

Genotyping of *E. histolytica*

To determine the strains of *E. histolytica* among HIV-1-infected Japanese patients, genotyping of *E. histolytica* was performed in patients who were PCR positive. The PCR method was used for the first time in our clinic for the diagnosis of amebiasis in December 2008, and since then 14 patients had been diagnosed as IA based on a positive PCR. For the PCR, DNAs were extracted from various biological specimens (e.g., stool, colon wash and punctuate-exudate) by using QIAamp DNA stool Mini Kit (Qiagen, Valencia, CA). Polymerase chain reactions were performed with specific sets of primers designed to target each of 6 loci (D-A, S-Q, R-R, A-L, S^{TGA}-D, and N-K) of tRNA-linked polymorphic short tandem repeats (STR), as described previously [21]. The PCR product was sequenced by ABI 3130XL Genetic Analyzer (Applied Biosystem, Foster city, CA) in both forward and reverse directions. Phylogenetic analysis and genotyping were performed as described previously [22].

Statistical analysis

Differences in patients' characteristics and clinical features were examined using the chi-square test or nonparametric test. The cumulative risk for recurrence was analyzed by the Kaplan-Meier method, and differences were tested by the log-rank test. The Cox proportional hazards model was used to assess the impact of luminal treatment on the recurrence rate after adjustment for other factors. The hazard ratio and 95% confidence interval were calculated. *P* values less than 0.05 were considered to denote statistical significance. All statistical analyses were performed using the Statistical Package for Social Sciences (SPSS Inc., Chicago, IL).

Results

Clinical data and response to treatment

IA was diagnosed in 170 HIV-1-infected cases between April 1997 and March 2010 (including amebic colitis, n = 102; ALA, n = 63; and perianal abscess, n = 5, Table 1). Thirty-three patients had two of the above three clinical forms of IA. All patients were males and 164/170 (96.5%) were MSM. High rates of positive TPHA (*Treponema pallidum* hemagglutination assay) (71.2%) and HBV exposure (HBs antigen-positive, HBs antibody-positive, or HBc antibody-positive) (60.0%) were observed. No significant differences were seen in CD4 counts, HIV-1 loads, coexisting AIDS definite disease and the proportion of patients treated with antiretrovirals, suggesting that HIV-induced immunocompromised status did not have an impact on the clinical presentation of amebic infection, in agreement with previous data [12]. In cases of amebic colitis (n = 102), diarrhea (69.7%) was the most common symptom followed by dysentery (55.9%) (Table 2). Fever (>37.5°C) was seen in only 20 patients (19.6%), including 5 cases with perforative peritonitis. In cases with ALA (n = 63), fever (95.2%) was the most common symptom followed by abdominal pain (55.6%). Diarrhea (46.0%) and dysentery (19.0%) were only seen in less than half of ALA cases. Single abscess (72.6%) was identified in most cases. Liver abscesses were seen more frequently in the right lobe (70.5%) than the left (9.8%). Nine patients (14.3%) had pleuritis (considered a co-existing disease), as well as abscesses in the right lobe, and 7 of these presented chest pain. Comparison of physical and laboratory data showed higher peak body temperature (BT), leukocyte count and C reactive protein (CRP) in ALA cases (Table 2) and perforative peritonitis cases (data not shown) compared with colitis cases, indicating that high fever, leukocytosis and high CRP could be the signs of extraluminal amebiasis. It is reported that high fever and leukocytosis are also common in ALA patients free of HIV-1 infection, though both parameters were unusually associated with simple amebic colitis [23]. In ALA cases, however, leukocyte count correlated positively with CD4 count (data not shown in tables: Pearson product-moment correlation coefficient 0.36, p value 0.004) and negatively with HIV-RNA load (Pearson product-moment correlation coefficient -0.28, p value 0.03), but CRP correlated neither with CD4 count nor HIV-RNA load (CRP-CD4, $p = 0.81$, CRP-HIV-RNA, $p = 0.32$). There were also no correlations between CD4 count, HIV-RNA load, BT, leukocyte count or CRP and abscess size or number.

All patients were treated with metronidazole (750 mg t. i. d. for 10 days) for IA, with the exception of two who were treated with tinidazole (2 g q. d. for 3 days). Complete remission of all IA symptoms was observed in 165 patients including the two treated with tinidazole. Five cases died within six months after diagnosis of IA; two from complications related to amebic colitis (one peritoneal perforation and one gastrointestinal bleeding), one from malignant lymphoma, one from *Pneumocystis jirovecii* pneumonia, and one from pulmonary thrombosis. The overall mortality rate was 3% in this study, which was comparable to those reported in non-HIV cases [2,23].

Recurrence after treatment

Luminal agents; paromomycin and diloxanide, are not approved in Japan, and they were not always available in our facility during the study period. After completion of IA treatment with metronidazole or tinidazole, luminal agents were administered when available. Consequently, 83 cases were treated with luminal

Table 1. Patient demographics, state of HIV, and serological markers.

	Colitis (n = 102)[1]	ALA (n = 63)[2]	Perianal abscess (n = 5)[3]	All (n = 170)	*P* value[4]
Age (years) [IQR]	38 [32–43]	37 [31–44]	45	38 [31–44]	0.58
Male sex (%)	102 (100)	63 (100)	5 (100)	170 (100)	–
Homosexual (%)	96 (94.1)	63 (100)	5 (100)	164 (96.5)	0.053
Past History of amebiasis (%)	16 (15.7)	9 (14.3)	1 (20.0)	26 (15.3)	0.81
CD4 count (/μl)	262 [98–398]	271 [123–411]	58	269 [107–403]	0.84
HIV-RNA (log copies/ml)	4.60 [3.89–5.32]	4.66 [3.91–5.11]	5.04	4.66 [3.93–5.28]	0.70
AIDS (%)	18 (17.6)	8 (12.7)	2 (40.0)	28 (16.5)	0.40
ART initiated (%)	18 (17.6)	11 (17.5)	1 (20.0)	30 (17.6)	0.98
TPHA test positive (%)	77 (75.5)	40 (63.5)	4 (80.0)	121 (71.2)	0.10
HBV exposure (%)	59 (57.8)	41 (65.1)	2 (40.0)	102 (60.0)	0.36
HCV Antibody positive (%)	3 (2.9)	3 (4.8)	0 (0)	6 (3.5)	0.42

Data are median [interquartile range: IQR] or number (percentage) of patients.
[1]5 cases of perforative peritonitis are included as co-existing diseases. Four cases were diagnosed coincidentally by colonoscopy in asymptomatic patients.
[2]31 cases of colitis, 1 case of perianal abscess, 9 cases of pleuritis, and 2 cases of peritonitis are included as co-existing diseases.
[3]1 case of colitis is included as co-existing diseases.
[4]Chi-square test or non-parametric test was performed for data of colitis and ALA.
UD: undetectable, ART: anti-retroviral therapy, TPHA test: *Treponema pallidum* Hemagglutination Assay test, HBV exposure: HBsAg-positive or HBsAb-positive, and/or HBc-Ab positive.
doi:10.1371/journal.pntd.0001318.t001

agents; 38 cases with promomycin (500 mg t. i. d. for 10 days) and 45 cases with diloxanide furoate (500 mg t. i. d. for 10 days). No significant differences were seen in patients' characteristics, including HIV-1-induced immunocompromised status, serological markers of other STD, and clinical forms and severity of amebiasis between the 83 cases with luminal treatment and 82 cases who did not receive such treatment (Table S1). The median follow-up period after completion of metronidazole or tinidazole treatment was 50 months (inter quartile range: 19–85) in those who received luminal treatment, and 43 months (inter quartile range: 23–98) in those without.

Table 2. Clinical features of amoebic colitis and ALA.

	Colitis (n = 102)	ALA (n = 63)	*P* value
Symptoms			
Diarrhea (%)	71/102 (69.6)	29/63 (46.0)	0.003
Dysentery (%)	57/102 (55.9)	12/63 (19.0)	<0.001
Abdominal pain (%)	23/102 (22.5)	35/63 (55.6)	<0.001
Chest pain (%)	0/102 (0.0)	7/63 (11.1)	<0.001
Peak BT (°C) [IQR][3]	36.8 [36.5–37.4]	39.0 [38.8–39.5]	<0.001
WBC (/μ l) [IQR][3]	5,830 [4490–7580]	11,760 [9460–15170]	<0.001
CRP (mg/dl) [IQR][3]	0.62 [0.16–3.02]	19.15 [10.53–24.75]	<0.001
Frequency of diarrhea[1]			
≤ 5 times/day (%)	63/101 (62.4)	–	
6–10 times (%)	26/101 (25.7)	–	
≥ 11 times (%)	12/101 (11.9)	–	
Size of abscess (mm)	–	59 (10–180)	
Location of abscess[2]			
Right lobe only	–	43/61 (70.5)	
Left lobe only	–	6/61 (9.8)	
Both lobes	–	12/61 (19.7)	
Number of abscesses[1]			
Single (%)	–	45/62 (72.6)	
Multiple (%)	–	17/62 (27.4)	

[1]Data of one case were not available.
[2]Data of two cases were not available.
[3]Data are median [interquartile range: IQR] or number (percentage) of patients.
BT: body temperature, WBC: White Blood Cell counts, CRP: C reactive protein.
doi:10.1371/journal.pntd.0001318.t002

Within the 12-month post-metronidazole treatment period, recurrence of IA was noted in only two patients who did not receive luminal treatment, suggesting reactivation of residual cysts of *E. histolytica* (Figure 1). However, during the entire follow-up period, six in each group experienced recurrence of IA, with no significant difference in the recurrence frequency by the log-rank chi-square test. Multivariate analysis showed that recurrence did not correlate with past history of IA, CD4 count, TPHA, HBV exposure (HBs antigen-positive or HBs antibody-positive), or the presence of extraluminal IA disease (Table 3). However, a positive HCV antibody was significantly associated with IA recurrence. Recurrence also tended to occur in those who acquired new syphilis infection during the follow-up period, though the difference did not reach statistical significance.

Genotypes of *E. histolytica*

Genotyping of *E. histolytica* was performed in samples obtained from 14 patients between December 2009 and March 2010 (colitis, n = 8; ALA, n = 4; colitis and ALA, n = 1; and perianal abscess, n = 1; Table S2). Eleven different genotypes were recognized, including five genotypes (J8, J12, J13, J20, and J23) identified previously in Japan [22], and six newly recognized genotypes (J24-J29). There was no significant relation between *E. histolytica* genotype and clinical presentation.

Discussion

In the present study, retrospective analysis of the medical records of 170 patients with HIV-1-infection and IA showed no

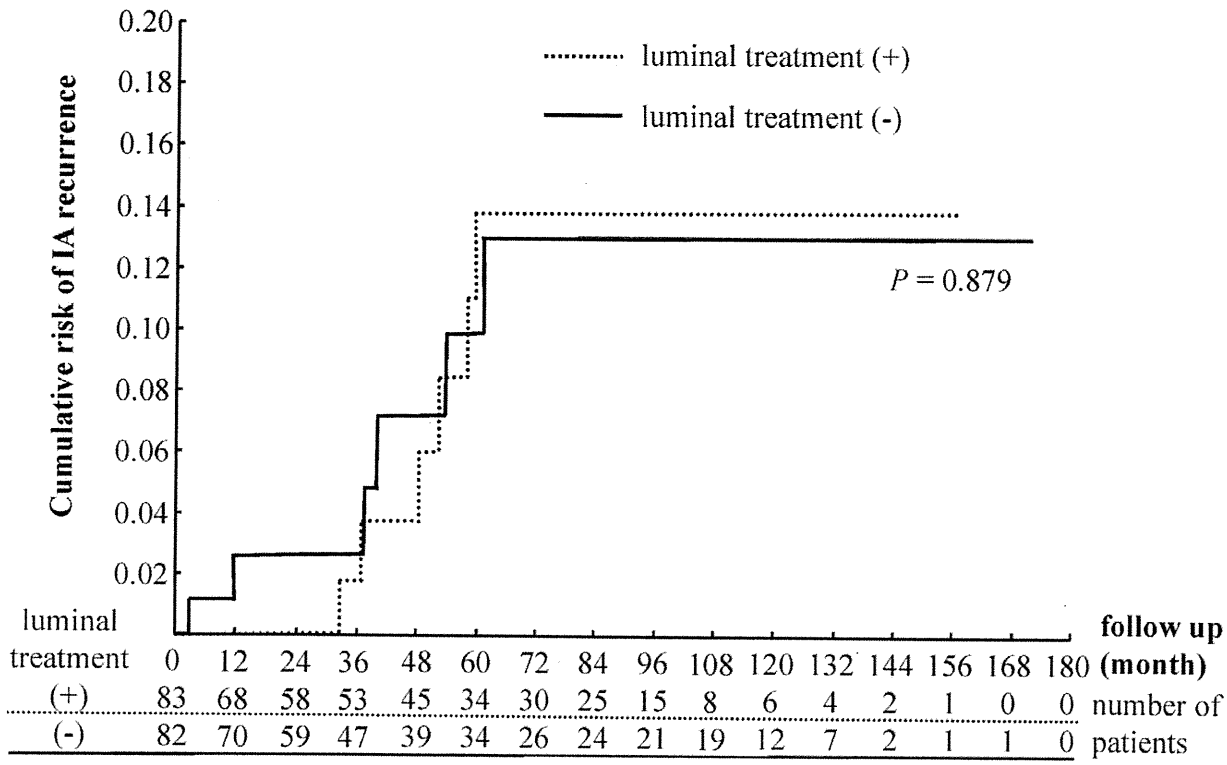

Figure 1. Kaplan-Meier estimates of time to IA recurrence. Cumulative probability of IA recurrence after completion of metronidazole or tinidazole treatment with or without subsequent luminal treatment.
doi:10.1371/journal.pntd.0001318.g001

impact for HIV-1-induced immunocompromised status on the clinical forms of amebiasis. The physical and laboratory findings showed that high fever, leukocytosis and high CRP correlated with extraluminal diseases of amebiasis. In ALA cases, however, leukocyte count correlated positively with CD4 count and negatively with HIV-RNA load, indicating that CRP is more sensitive marker for the detection of the extraluminal diseases in advanced immunocompromised patients.

Only five patients died after the diagnosis of IA; two from IA complications and three from other causes. The results indicate excellent outcome for HIV-1-infected individuals with uncomplicated amebiasis treated with metronidazole or tinidazole, in agreement with previous reports on HIV and non-HIV cases [2,11,12,20,23]. Based on conventional wisdom and written opinion, adequate management of IA should include treatment with a luminal agent following metronidazole or tinidazole treatment, in order to eradicate residual cysts of *E. histolytica* due to the high rate (40–60%) of luminal colonization [2,23–27]. On the other hand, the results of longitudinal observational studies indicated that asymptomatic cyst carriers rarely develop IA, and

Table 3. Multivariate analyses for factors associated with frequency of recurrence.

	No recurrence (n = 153)[1]	Recurrence (n = 12)	Hazard ratio (95.0% CI)	*P* value
Past history of IA[2] (%)	24 (15.7)	2 (16.7)	0.914 (0.186–4.478)	0.911
CD4 counts <200[2] (%)	57 (37.3)	3 (25.0)	0.385 (0.101–1.470)	0.162
TPHA test positive[2] (%)	108 (70.6)	10 (83.3)	2.435 (0.501–11.827)	0.270
HBV exposure[2] (%)	92 (60.1)	7 (58.3)	1.248 (0.364–4.277)	0.725
HCV Antibody positive[2] (%)	3 (2.0)	2 (16.7)	7.664 (1.369–42.890)	0.020
Extraluminal disease[2] (%)	66 (43.1)	4 (33.3)	0.559 (0.163–1.921)	0.356
No luminal agent (%)	76 (49.7)	6 (50.0)	1.070 (0.322–3.559)	0.912
Syphilis during follow-up period (%)	33 (21.6)	7 (58.3)	3.332 (0.961–11.547)	0.059

[1]Five patients died within 6 months from disease onset and their data were excluded from analysis.
[2]Status at diagnosis of IA.
doi:10.1371/journal.pntd.0001318.t003